Organic waste: A bioresource for production of novel cellulose nanocomposites

Technical report

ANNIE FA CHIMPHANGO

Waste Research Development and Innovation Roadmap Research Report

5 MARCH 2021

science & innovation
Department:
Science and Innovation
REPUBLIC OF SOUTH AFRICA

UNIVERSITEIT STELLENBOSCH UNIVERSITY

CSIR
Touching lives through innovation

Organic waste: A bioresource for production of novel cellulose nanocomposites

Prepared for

Department of Science and Technology
Directorate Environmental Services
and Technologies
Private Bag X894, Pretoria,
South Africa, 0001

Council for Scientific and Industrial Research
Waste RDI Roadmap Implementation Unit
PO Box 395, Pretoria,
South Africa, 0001

Prepared by

Stellenbosch University
Private Bag X1
Matieland, 7602, South Africa

Author

Annie FA Chimphango

Contributors: Mr Regan Ceaser & Ms Fatimatu Bello (Students on the project)

Waste RDI Roadmap Grant Number: CSIR/IU/WRIU/2016/009

March 2021

EXECUTIVE SUMMARY

Organic wastes from agricultural fields and processes are available in abundance but currently have very low economic value, and their disposal is a cause of environmental concerns. However, the organic wastes' chemical composition renders them suitable feedstock for the production of high- value products in integrated biorefineries. Identifying optimal process conditions and novel methods for diversifying the functional properties of both the organic wastes and the bioproducts derived from them, would advance the development of sustainable integrated biorefineries with multiple economic and environmental gains to the agricultural industry and beyond (Figure I provides an integrated approach for obtaining high-value bioproducts from the agricultural residues including nanocelluloses, with new functionalities).

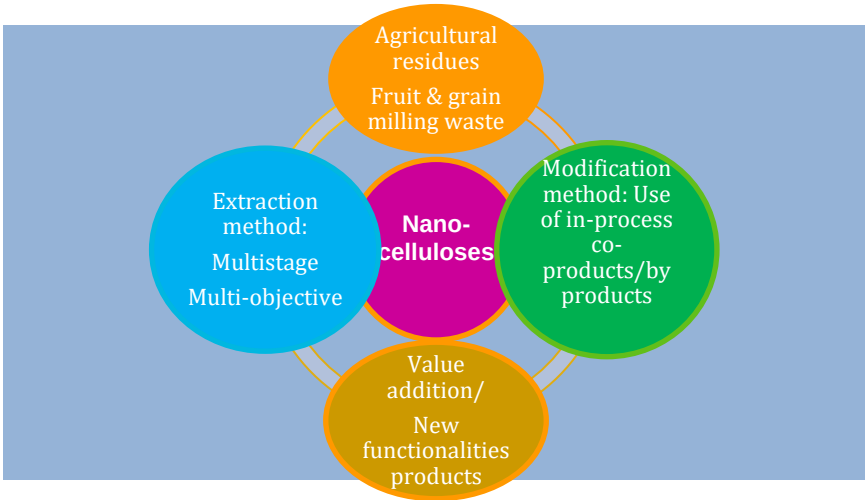

Figure I: Valorisation of agricultural residues to produce high-value co-products with advanced functionalities

The project aim was to add value to organic wastes in the form of residues from mango processing (peels, kernel and husks) and cereal field and processing (wheat straw and wheat bran). The residues were characterised for their physical characteristics and chemical compositions, which formed the basis for the development of suitable fractionation routes for the co-extraction of high-value bioproducts in a biorefinery set up. The specific objectives included the development and optimization of process conditions for the fractionation routes that could maximize the number and yields of high-value bioproducts from the wheat residues (Fig. II) and mango wastes (Fig III). The objectives were achieved through two research projects "**Comparative analysis of methods for producing nanocellulose from wheat straw and bran, with co-extraction of valuable products" and** "**Development of a process route for co-extracting nanocellulose and high-value-added products from mango waste"**. In both projects, the residues were valorised into hemicelluloses, lignin, polyphenols, and cellulose (which was further fractionated to produce nanocellulose), in multiple stages that were each optimized to increase yields and improve the functional properties.

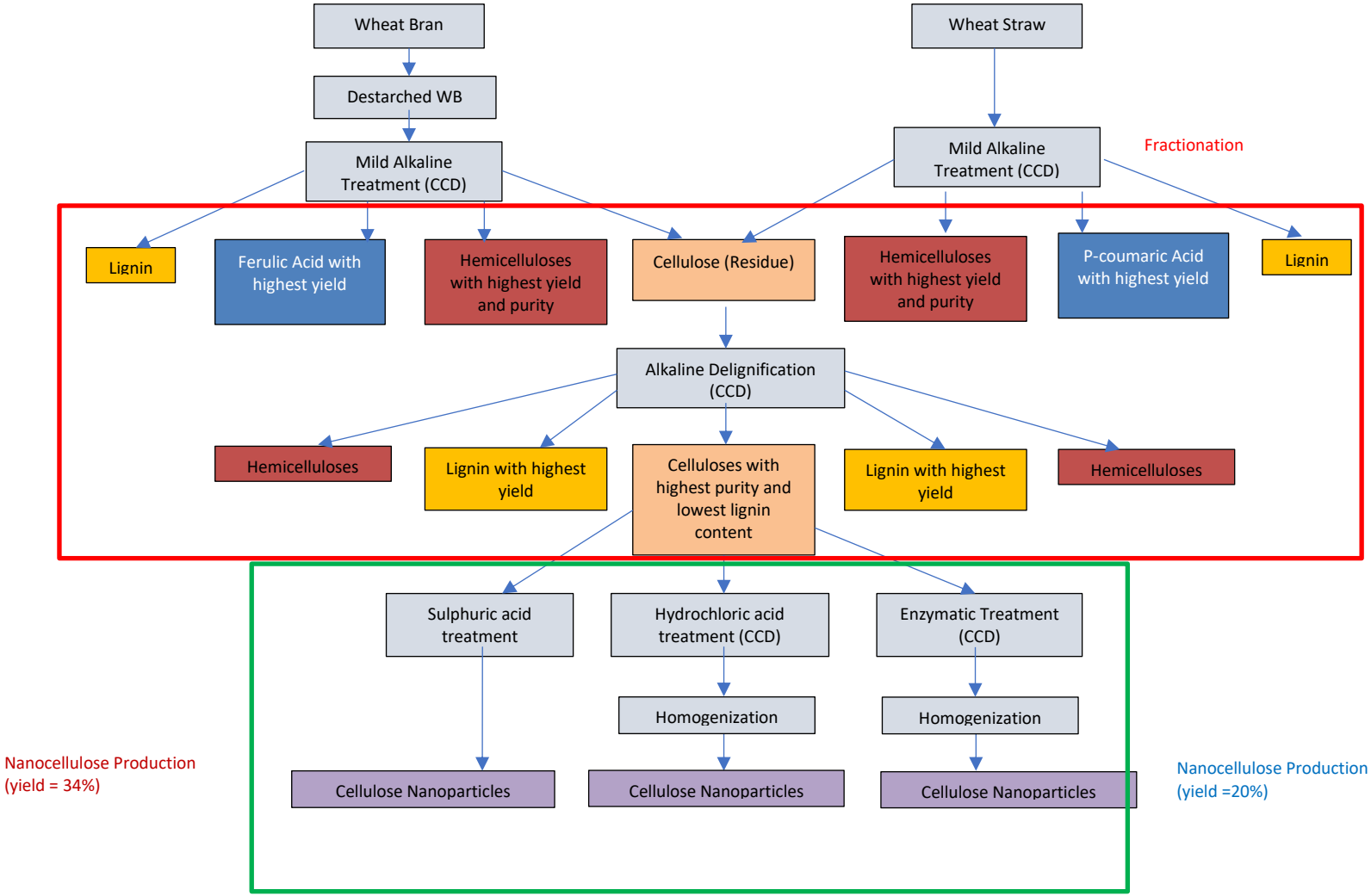

Figure II: Fractionation routes for valorization of wheat residues into high-value products. Note: CCD = Central composite designed experiment for optimization of process conditions

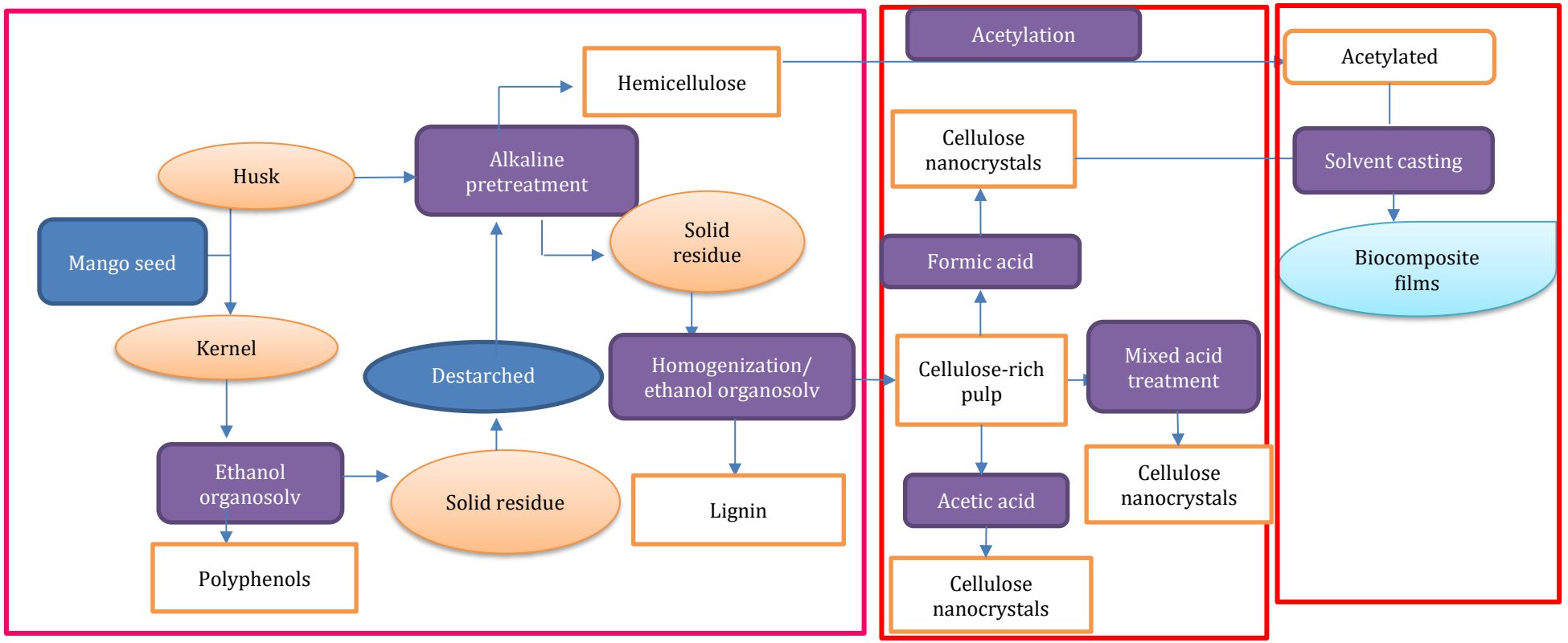

Figure III: Fractionation routes for mango waste valorization to produce high-value products. Each step in purple was optimized

The optimal conditions for the mild alkaline treatment (50 and 60 ºC and NaOH between 2.0 and 3.0 wt. %) of wheat residues (Fig II) targeted the removal of hemicelluloses and phenolic compounds, in particular, the *p*-coumaric acid, whereas, the optimal conditions of the wheat bran (~ 70 ºC with NaOH between 2 and 3 wt. %), targeted the removal of hemicelluloses and the phenolic compounds *(ferulic* acid). In both cases, the integrity of the cellulose-rich residues was preserved for lignin and nanocellulose production. The lignin-cellulose-rich residues were further subjected to the second stage, severe alkaline delignification process (Fig II) at the optimal conditions of ~10 wt. % NaOH for the wheat bran and ~12 wt. % NaOH for the wheat straw, both were performed for ~1.5 h at 121ºC. The delignification stage targeted the removal of lignin although the co-extraction of the residual hemicelluloses was unavoidable, while preserving the cellulose-rich residue for nanocellulose production,

The total yields for the hemicelluloses and lignin after the two-stage alkaline treatment, from the wheat straw ranged between 65- 80% and *p*-coumaric acid yield >40%, with an antioxidant activity > 80%. The process yielded >90% cellulose-rich residues from the wheat straw with a cellulose content >70%. The cellulose crystallinity >50% rendered the cellulose-rich residues suitable for nanocellulose production. On the other hand, the wheat bran residues were rich in hemicellulose (> 50%) and lignin (>90%) with a *ferulic* acid yield >60%. The cellulosic rich residues recovery from the wheat bran was > 80% but contained < 50% cellulose with > 30% and 5% residual hemicellulose and lignin, respectively. Therefore, the wheat bran cellulosic residues were suited for specialty nanocellulose production using the methods specified in Figure II.

The nanocellulose production from the wheat residues was by either hydrochloric acid (HCl) or enzymatic treatments that were chosen based on their potential positive attributes on the environment and the morphology and functional properties attained by the produced nanocellulose. The optimal conditions for the two methods were 4 M HCl, ~7.0 h and between 110 and 115ºC for the HCl-based method, and 4.64 h, FibreCare of 75 ECU/g and Viscozyme of 10.8 FBG/g for the enzymatic method at 50 ºC (Ceaser & Chimphango, 2021). The yields from the two methods were comparable (~20%) but less than the yield (34%*)* obtained using sulphuric acid treatment (Fig II). However, the nanocellulose obtained had a maximum thermal decomposition temperature > 40 °C higher than the sulphuric acid nanocellulose (SCN). The surface charge and the morphology of the nanocelluloses from the hydrochloric acid (HCN) and enzymatic treatments (ECN) were similar except for the particle size distribution defined by the polydispersity index. Notably, the enzymatic method was 1.5 times faster to produce the same yield of nanocellulose than the HCl method. The nanocellulose produced were classified as cellulose nanofibers (CNFs) that were relatively stable colloids (based on the Zeta potential~– 16 mV) (Ceaser & Chimphango, 2021). However, due to the differences in the morphology, the end-use industrial applications could be different (Ceaser & Chimphango, 2021).

In mango waste valorization, an alkaline treatment was developed for the fractionation of the mango seed husk into hemicelluloses of varying compositions to tailor-make their end-use in the formulation of biocomposites for food packaging applications. The optimal validated extraction conditions were identified to be 1.92 M NaOH, 86 °C, and 3.84 h, which gave hemicellulose yield and purity ~ 50 and >60, respectively, having a xyloglucan (XGN) / xylan (XLN) ratio of 0.13, with 12% uronic acids and ~17% associated lignin. The hemicelluloses would suit the formulation of thermally stable (290 °C) biocomposites films (Bello & Chimphango (unpublished)). However, the hemicellulose fractions with varied xyloglucan (XGN) and xylan (XLN) ratios (0.13-0.47) could be obtained by varying the extraction conditions, which could lead to diversified applications.

The mango seed kernels were rich in polyphenols, hemicellulose, and starch but had limited cellulose and lignin contents (both < 5.0%), thus, were not suitable for nanocellulose production. The optimal conditions for polyphenol extractions (44% v/v ethanol and 54 °C) gave a polyphenol extract yield of 20.83% with a total polyphenolic and scavenging activity of 4296.70 mg GAE/100 g and 82.69%, respectively. The solid residue was rich in hemicellulose and starch (20.11% and 43.67% respectively). At the optimal alkaline conditions (1.5 M NaOH, 44 ^{o}C, and 3 h), for the extraction of hemicellulose extraction from the destarched polyphenol-extracted residue, the hemicellulose yield, total polyphenolic content, antioxidant activity, lignin, and uronic acid contents were ≥57%, 2150 mg GAE/100g, 56%, ~5.5%, and 14%, respectively.

The husk's cellulose content of ~50% rendered the husks a suitable feedstock for nanocellulose production. The husks, pretreated in an alkaline were subjected to an organosolv process (Fig. III) before being subjected to various acid treatments for nanocellulose production, which was classified as nanocrystals (CNC). A comparative analysis of three acids (sulphuric acid, acetic acid and formic acid) (Fig III) showed that the nanocellulose yields for formic acid (> 60%) and acetic acid when assisted with homogenization (>70%), were higher than those obtained using sulphuric acid (~38%). The nanocellulose from sulphuric acid (SCNC) and formic acid (FCNC) had similar particle sizes (< 30 nm), whereas, the sizes for the acetic acid nanocelluloses (ACNC) were relatively higher (~ 40 nm). Notably, the FCNC and ACNC were spherical and more thermal stable (> 350 °C) than SCNC (<300 °C). However, there was no difference in crystallinity (> 60 %) among the CNCs.

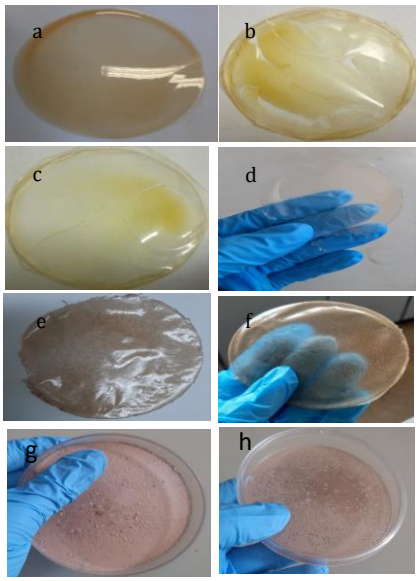

Figure IV. Biocomposite films from (a) xyloglucan, (b) xylan, (c) combination of xyloglucan and xylan (without plasticizer), (d), combination of xyloglucan and xylan (with plasticizer), (e) mango seed husk hemicellulose (without plasticizer) and (f) mango seed husk hemicellulose (with plasticizer) (g) mango seed husk hemicellulose with. 10% and (h) 40% formic acid generated nanocellulose products.

Films were produced from the hemicelluloses obtained from the alkaline pretreatment process (Fig IV). The films formed with acetylated hemicelluloses before being combined with nanocellulose produced self-supporting and relatively hydrophobic (water contact angle >80^{o}) biocomposites (Fig. IV). The mechanical properties of the biocomposite compared well with those of the commercial low-density polyethylene (LDPE) that are used in food applications. The tensile strength, Young's Modulus and contact angles were approximately 11 MPa, 240 MPa and >80^{o}, respectively. The mechanical properties of the biocomposite improved with the addition of a plasticizer.

The two projects demonstrated the potential of two stepwise fractionation routes, which, with optimization of each step, could potentially produce seven functional high-value co-bioproducts (cellulose, hemicellulose, lignin, pectin, polyphenols, proteins, and starch) from wheat residues and mango processing waste in high yields but only five bioproducts (lignin, polyphenols, hemicelluloses, cellulose and nanocellulose) were targeted in this project. Further work is needed to explore more applications of the bioproducts and assess the economic viability and overall sustainability of the fractionation routes.

TABLE OF CONTENTS

TABLES

FIGURES

ABBREVIATIONS AND ACRONYMS			
ACNC	Acetic acid nanocrystals/nanocellulose	M_{CA}	Mass of crucible and Ash
AD	Acid detergent	M_{cr}	Mass of crucible and dry residue
ADL	acid detergent lignin	M_D	Mass of oven dry sample
ADF	Acid detergent fibre	MEng	Master of Engineering
AHFN	Acetylated hemicellulose with nanocellulose	M_F	Mass of flask
AIL	Acid insoluble	MF_{EX}	Mass of oven dried flask with extractives
ANOVA	Analysis of Variance	MHH	Mango seed husk hemicellulose
ASL	Acid soluble	min	Minute
^oC	Degree Celcius	mL	millLitre
CCD	Central composite design	M_P	Mass of protein
CrI	Crystallinity Index	MPa	Mega Pascals
CNC	Cellulose nanocrystals/ nanocellulose	MSD	mass spectrometer detector
Conc	Concentration	mV	mill Volts
CNF	Cellulose nanofibres	M_w /Mw	Mass of sample/ Molecular Weight
CP/MAS NMR	cross polarization and magic angle spinning Nuclear Magnetic Resonance	N	Normality
CSIR	Council for Scientific and Industrial Research	N/A	Not Applicable
CXLN	Commercial xylan	NaOH	Sodium Hydroxide
DAFF		NDF	neutral detergent fibre
dm	Dry matter	NFC	Nanofibrillated Cellulose
DMA		NMR	Nuclear Magnetic Resonance
DEMAC	Dimethyl acetamide	NREL	National Renewable Energy Laboratory
DMF	Dimethylfomamide	NRF	National Research Foundation
DMSO	dimethyl sulphoxide	od	oven dry

DPPH	2,2-diphenyl-1-picrylhydrazy	OD	Optical density/ oven dry
DS/*DS*	Degree of substitution/ D-Glucose unit	P	Pressure
DST/ DSI	Department of Science and Technology/ Innovation	Pa	Pascal
ε	Biomass emissivity	Ph.D.	Doctor of Philosphy
ECN	Enzymatic nanocellulose	PSS	Polymer standard service
ECU	endo-1,4-β-glucanase unit	rpm	Revolution per minute
ELS	Evaporative light scattering	RSM	Response surface methodology
FBG	fungal β-glucanase units	SA	Severe Alkaline
FCNC	Formic acid cellulose nanocrystals	SAWB	Severe alkaline wheat bran
FD	Freeze dried	SAWS	Severe alkaline wheat straw
FTIR	Fourier Transfer Infrared Spectroscopy	SCN	Sulphuric acid nanocellulose
g	gram	SCNC	Sulphuric acid nanocellulose/ nanocrystals
GAE	Gallic acid equivalent	sec	Seconds
GC-MS	Gas chromatography-mass spectrometer	SEM	Scanning Electron Microscopy
GPC	Gel permeation Chromatography	SFCNC	Spherical formic acid cellulose nanocrystals
h	Hour	T	temperature
HCl	Hydrochloric acid	t	Time
HCN	Hydrochloric acid nanocellulose	TEM	Transmission electron microscopy
HMF	5-hydroxymethylfurfural	TGA	Thermogravimetric Analysis
HPLC	high-performance liquid chromatography	UMH	unbleached mango husks
HSHO	high shear homogenization assisted-organosolv	US	United State of America
A, B, C, D	Volumes of chemicals A, B, C & D	UV_{wave}	Ultra Violet Absorbance @ 240 nm

LAP	Laboratory Analytical Procedure	V_b , V_f; V_{ts}	Volume of titrate blank (b) and of filtrate (f) and test sample (ts)
LDPE	Low density polyethylene	WB	Wheat bran
m	mass	WS	Wheat straw
M	Molar	X	Independent variable
MA	Mild alkaline	XGN	Xyloglucan
M_{Ac}	Mass of crucible and ash	XLN	Xylan
MAWB	Mild alkaline wheat bran	XRD	x-ray diffraction
MAWS	Mild alkaline wheat straw	Y	Response variable
M_c	Mass of crucible	ZP	Zeta Potential

1 Introduction

Organic wastes obtained from agricultural fields and agro-processes are available in abundance but currently have very low economic value. Furthermore, the disposal of the organic waste is a cause of environmental concerns such as greenhouse gas emissions (Xu *et al.*, 2018; Joglekar, Pathak & Mandavgane, 2019). The organic wastes' chemical composition consists of various compounds, which if selectively extracted, can create additional high-value chains. Most of the available biomass fractionation methods are not optimized for non-woody materials and often consider limited products (Durán *et al.*, 2018). Therefore, identifying the optimal process conditions specific for fractionation of the agricultural-based organic wastes would advance the development of sustainable integrated biorefineries with multiple economic and environmental gains to the industry (Moniz *et al.*, 2015; Cebreiros, Guigou & Cabrera, 2017).

Lignocellulosic materials are fractionated by various methods including, alkaline, organosolv, ionic liquids, hydrothermal, and super critical methods (Agbor *et al*., 2011) that target mainly the isolation of components such as cellulose, hemicellulose and lignin without considering other by-products and co-products as reflected in the chemical compositions (Table 1 for wheat residues). Noteworthy, the field and processing residues from fruits and cereals are rich in a variety of structural and functional compounds that could create additional high-value chains (Tunchaiyaphum, Eshtiaghi & Yoswathana, 2013). However, the total utilization of the organic wastes is a challenge because most of the functional compounds degrade under the processing conditions that are optimized specifically for isolating structural compounds such as celluloses, hemicelluloses and lignin. Therefore, a strategic configuration of the process steps and optimization of the conditions are required to enable co- extraction of compounds with different optimal conditions, which would increase the number of functional bioproducts and leading closer to total organic waste utilization.

An integrated approach to organic waste valorization (Figure 1) provides the basis for increasing the value that can be obtained from the agricultural residues. The key features in the approach include the selective extraction of high-value products including nanocelluloses, and the modification of the products to introduce new functionalities.

The functional compounds (Table 1), including the hydroxycinnamic acids (*ferulic* acid and *p*-Coumaric) make up a small percentage of the total biomass composition but both have much higher commercial value than the traditional fractionation products. *Ferulic* acid and *p*- Coumaric acid have been of interest due to their antioxidant properties, which are in high demand in the pharmaceutical, food industry and cosmetic industries, among others. In the pharmaceutical industry, *ferulic* acid is used as an additive for reducing liver cholesterol and coronary diseases (Ou *et al.*, 2007). Whereas, *p*-Coumaric acid is used as an additive to reduce the risk of stomach cancer (Max *et al*., 2009). In addition, *ferulic* acid is a precursor for high-value products such as vanillin (Tapin *et al*., 2006) and, *p*-Coumaric acid a precursor for *p*-hydroxybenzoic acid (Jiang *et al*., 2016b).

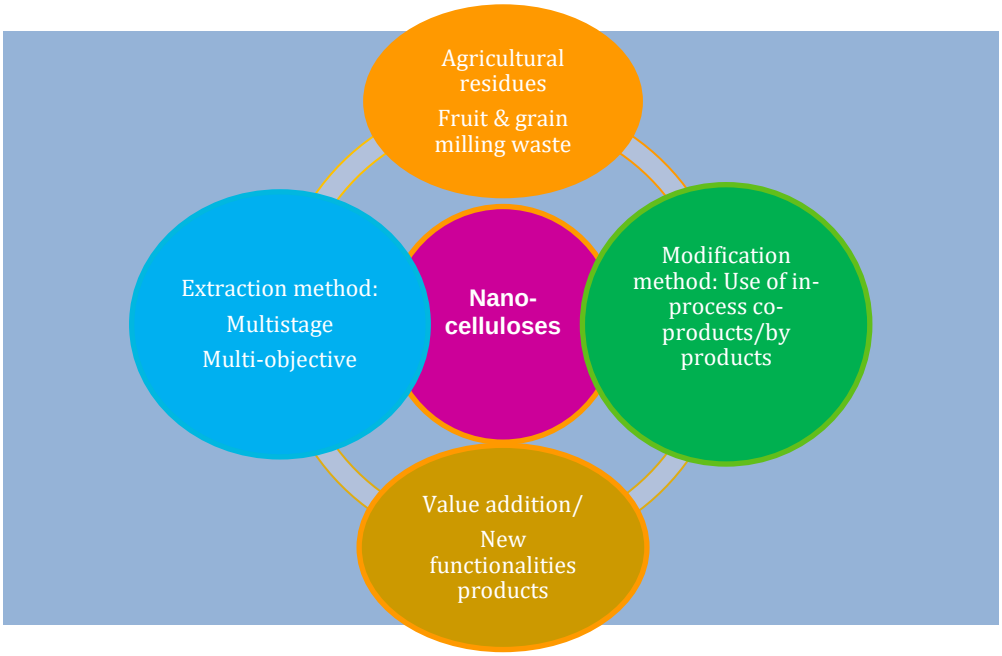

Figure 1. Valorization of agricultural residues to produce high-value co-products with advanced functionalities

In comparison with the composition of other related materials (Table 2), cotton has the highest cellulose content (>80%) (Sun & Cheng, 2002), while the cellulose content of the agricultural residues ranges from 30-40% (Table 2). However, there is a limited number of products that can be obtained from pure cotton in a biorefinery context compared to the agricultural residues. Moreover, the cellulose content of the agricultural residues can be enhanced through pretreatments(Henrique *et al.*, 2013).

The project aim was to develop and validate biorefinery process routes for optimal fractionation of the grain and sub-tropical fruit process wastes and further modify and evaluate the functional properties of the fractionated products. The research objectives were addressed in two research projects at Masters and Ph.D. levels with the titles "**Comparative analysis of methods for producing nanocellulose from wheat straw and bran, with co-extraction of valuable products" and** "**Development of a process route for co-extracting nanocellulose and high-value-added products from mango waste"**, respectively.

Table 1 Chemical composition of wheat straw and bran on dry matter (dm) basis.

Components	Wheat Straw (% dm)	Wheat Bran (% dm)	Reference
Cellulose	38.5 – 45.7	10.7 – 20.8	(Kaushik & Singh, 2011; Barman *et al.*, 2012; Merali *et al.*, 2013; Cripwell *et al.*, 2015)
Hemicelluloses	24.0 – 38.2	33.5 – 58.2	(Lee *et al.*, 2007; Favaro, Basaglia & Casella, 2012; Janker-Obermeier *et al.*, 2012; Merali *et al.*, 2013)
Lignin	7.9 - 27.2	2.7 – 12.1	(Favaro, Basaglia & Casella, 2012; Tutt, Kikas & Olt, 2012; Jaisamut *et al.*, 2013; Merali *et al.*, 2013)
Starch	2.7	11.0 – 38.9	(Barman *et al.*, 2012; Cripwell *et al.*, 2015; Onipe, Jideani & Beswa, 2015)
Protein	1.9 – 5.7	9.6 - 18.6	(Lee *et al.*, 2007; Khan & Mubeen, 2012; Onipe, Jideani and Beswa, 2015)
Extractives	9.4	N/A	(Barman *et al*. 2012; Merali *et al.* 2013)
Ash	3.57 – 9.9	3.2 – 11.6	(Tahir *et al*., 2002; Saleem Khan & Mubeen, 2012; Tutt, Kikas & Olt, 2012; Sánchez-Bastardo, Cocero & Alonso, 2013)
Ferulic Acid	0.11-0.25	0.40-1.5	(Sun, Lawther & Banks, 1995; Buranov & Mazza, 2009; Sipponen *et al.*, 2014; Boz, 2015)
p-Coumaric Acid	0.20-0.42	0.02-0.26	(Buranov & Mazza, 2009; Ou *et al.*, 2012; Merali *et al.*, 2013; Sipponen *et al.*, 2014)

N/A represents not available

Table 2 Compositions of lignocellulose quantified in different agricultural residues

Biomass source	Cellulose (%)	Hemicellulose (%)	Lignin (%)	Pectin (%)	Polyphenols (mg/g)	Reference
Barley straw	34.8	27.9	14.6	–	–	(Sun, 2010)
Coastal Bermuda grass	25.0	35.7	6.4	–	–	(Sun & Cheng, 2002)
Corn cobs	43.2 – 45.0	31.8 – 35.0	14.6 – 15.0	–	–	(Sun & Cheng, 2002; Sun, 2010)
Corn stover	29.7	25.0	12.3	–	–	(Liu-Xuan, 2016)
Cotton seed hairs	80.0 – 95.0	5.0 – 20.0	0	–	–	(Sun & Cheng, 2002)
Esparto	35.8	28.7	17.8	–	–	(Sun, 2010)
Grasses	25.0 – 40.0	35.0 – 50.0	10.0 – 30.0	–	–	(Sun & Cheng, 2002)
Leaves	15.0 – 20.0	80.0 – 85.0	0	–	–	(Sun & Cheng, 2002)
Maize stems	38.5	28.0	15.0	–	–	(Sun, 2010)
Mango husk	50.0 – 55.0	20.6 – 21.2	9.0 – 25.5	–	–	(Henrique *et al*., 2013; Cordeiro *et al*.., 2014, Andrade *et al*., 2016)
Mango kernel	25.2	34.1	15.0	0.8	–	(Kaur *et al*., 2004; Nwadiogb *et al*., 2015)
Mango peel	38.3	13.9	27.9	20.0 – 35.0	55 – 110	(Ajila *et al*., 2007a Yingkamhaeng & Sukyai, 2014 ; Banerjee *et al*., 2016)
Nutshell	25.0 – 30.0	25.0 – 30.0	30.0 – 40.0	–	–	(Sun & Cheng, 2002)
Oil palm fiber	40.2	32.1	18.7	–	–	(Sun, 2010)
Pear pomace	32.4	20.2	25.9	–	–	Rabetafika *et al*., 2014
Rape straw	37.6	31.4	21.3	–	–	(Sun, 2010)
Sugar beet pulp	18.4	14.8	5.9	27.1	–	(Sun, 2010)
Sugar cane bagasse	39.2 – 43.6	27.7 – 28.7	19.4 – 27.7	–	–	(Sun, 2010; Teixeira *et al*., 2011)
Switch grass	45.0	31.4	12.0	–	–	(Sun & Cheng, 2002)
Wheat straw	30.0 – 38.6	21.0 – 50.0	11.0 – 22.9	–	–	(Sun & Cheng, 2002; Sun, 2010; Khan & Umarah Mubeen, 2012)

1.1 Objectives

The specific objectives for the included:

1. Identifying optimal fractionation and recovery processes from literature for isolation of cell wall components into the most economical product portfolio comprising of celluloses, hemicelluloses, lignin with pectin, organic acids, and polyphenols as by-products and co-products from grain and sub-tropical fruit process wastes.
2. Experimental validation of the identified process route(s) by determining appropriate conditions for fractionation of the products and characterization of the physical and functional properties of the fractions.
3. Based on documented methods, develop innovative methods (including the use of a combination of physical, chemical and biological methods) for the selective production of nanocellulose from the cellulosic component of the waste.
4. Technical evaluation of the methods for functionalisation of nanocelluloses for the food packaging industry

1.2 Research Questions

The research questions addressed in the project included:

- What are the process routes for the fractionation of the organic waste to obtain the most economic product profile?
- What major quality attributes should be used for evaluating the fractionation products, co-products, and by-products from the grain milling and sub-tropical fruit process residues for purposes of integrating them in nanocellulosic composites?
- What methods or method combinations are suitable for selective isolation of nanocellulosic materials from the milling grain and sub-tropical fruit process residues?
- What methods or method combinations should be used to produce novel cellulose nanocomposites targeting food packaging?

1.3 Project tasks, deliverables, and milestones

The main tasks for the project (Table 3) included comprehensive literature review on fractionation and modification methods, which informed the selection of the methods for fractionating the different waste fractions from the two sources into high-value products. The outcomes of the literature review were compiled into two project proposals for the development and optimization of the fractionation routes for the wheat and mango wastes. Comprehensive characterization of the materials was performed to inform the potential products that can be extracted and the suitable fractionation methods. Statistically designed experiments, in particular, the central composite design (CCD) experiments (Statistica®) were implemented for optimizing fractionation conditions. The optimal conditions were found through desirability analysis. The fractionation conditions were validated to ascertain the repeatability and reliability of conditions. The products

generated were characterized for their structural features such as morphology and functionality as related to the presence of functional groups, thermal stability, hydrophobicity, and suitability for the formation of biocomposites that would suit food packaging.

Table 3 Main tasks and associated deliverables and milestones for the project

Tasks	Deliverables	Milestones
Literature review on fractionation and modification methods	Report on literature review and identification of research gaps	Research proposal
Experimental design and waste characterization	Chemical composition of the waste Compilation of potential product portfolios from the waste	Waste product profile
Development of biorefinery routes for organic waste.	Bio-refinery scenario simulations. Technical efficiency, socioeconomic impacts and sustainability	Business Model for waste biorefineries
Experimental validation of promising biorefinery routes.	Sourcing of organic waste samples Selection of process conditions Fractionation of samples using selected process conditions for the selected process/product combination Optimization of process conditions for fractionation of the products	Optimized conditions for fractionation
Production of nanocelluloses	Identification of methods or their combinations for producing nano-celluloses Production of nanocelluloses Characterization of nano-celluloses	Nano-cellulose methods are identified Defined yields, quality and functional properties
Production of nanocomposites	Production of nano-composites: Selection of optimal production conditions Quality assessments	Conditions for nano-composites production e.g. solid loading, temperature and time
Testing of the functionality of the nanocomposites in food packaging	Applicability of the nano-composites in food packaging is tested	Conditions for applying nano-composites to improve surface characteristics and functional properties

2 Research Approach and Experiments

The research questions were addressed through comparative analysis of the conventional routes and the developed fractionation routes for the raw materials to co-produce the high-value products from wheat and mango wastes that were tested in the two separate projects. The two projects are described in detail in the subsequent sections:

2.1 Project 1: Comparative analysis of methods for producing nanocellulose from wheat straw and bran, with co-extraction of valuable product

2.1.1 Background:

Wheat straw and wheat bran are mostly used in low economic activities such as feed for animals or are dumped in landfills. Both types of organic wastes have gained attention as feedstocks for integrated biorefineries due to their diverse chemical compositions (Table 1). These organic waste are potential sources for special compounds such as hemicellulose and hydroxycinnamic acids such as *p* coumaric acid and *ferulic* acid acid (Bataillon *et al.*, 1998; Pan *et al.*, 1998; Peng & Wu, 2010; Vijayalaxmi, Jayalakshmi & Sreeramulu, 2014). . The wheat straw composition renders the feedstock more suited for the extraction of lignin and cellulose for nanocellulose production (Sun *et al.*, 2005; Liu, 2017) than the wheat bran. However, the cellulose obtained from the wheat bran has potential for the production of specialty nanocellulose (Alemdar & Sain, 2008; Claes Nilsson, 2017) but with limitations in terms of yields.

The extraction of hemicelluloses, lignin and hydroxycinnamic acids from agricultural residues is made possible through mild alkaline treatments (Hosseinian and Mazza, 2009; Egüés *et al*., 2012; Jiang *et al*., 2016a)). Through the treatment, cellulose-rich residues containing some lignin are obtained in high yields and with improved crystallinity if the alkaline conditions are properly controlled (Karp *et al*., 2014). Therefore, optimizing of the mild alkaline process presents favourable conditions for co-producing hemicellulose, hydroxycinnamic acid, lignin and cellulose-rich residues (which can further be used for nanocellulose production).

Nanocellulose sources have included bleached cellulosic fibers or commercial cellulose fibers whereas, the use of other chemically produced cellulose fibers have received little attention. (Alemdar & Sain, 2008; Espinosa *et al.*, 2017). The nanocellulose production methods have mainly been sulphuric acid-based, which often, are associated with higher nanocellulose yields compared to alternative methods but with reduced thermal stability due to the presence of the sulphur groups (Cheng *et al*., 2017). Therefore, alternative methods such as hydrochloric acid (HCl) and enzymatic treatments have recently received much attention (Shibuya & Hayashi, 2008; Cheng *et al.*, 2017). A comparative analysis of the alternative methods with the conventional methods could provide a better understanding of the nanocellulose production mechanisms and functionality. In this project, an

alkaline-based fractionation process was developed, optimized and validated for the isolation of cellulose-rich residue hemicellulose, lignin, *ferulic* and *p*-coumaric acids. The fractionated products were characterised at each stage of the process (Fig. 2) to ascertain their functional properties. The lignin and cellulose-rich fractions were subjected to either hydrochloric acid or enzymatic hydrolysis to produce nanocellulose. The effectiveness of the two methods was compared with that of the conventional sulphuric acid method.

2.1.2 Production of hemicelluloses, lignin, and phenolic compounds

2.1.2.1 Materials and Methods

The wheat straw (WS) was obtained from NK Feeds in Paarl, whereas, the wheat bran (WB) was obtained from Eureka Mills, South Africa. The valorization of the organic wastes involved three stages, mild alkaline, severe alkaline, and mild acid or enzymatic treatments (Fig. 2). The mild alkaline treatment conditions were based on NaOH with concentrations ranging from 1.5 - 2.5 M NaOH with lower and upper extreme mild conditions of ~ 1.2 and 2.7 M NaOH (Table 4), respectively. The optimal conditions for the mild alkaline conditions (Fig 2) targeted the removal of hemicelluloses and phenolic compounds, in particular, the *p*-coumaric acid from wheat straw and *ferulic* acid from wheat bran (Fig. 2). The cellulose-rich residues recovered from the mild alkaline step were subsequently, subjected to the second stage, a severe alkaline delignification process, which targeted mainly the removal of lignin although hemicellulose co-extraction occurred. The treatments were performed at temperatures between 20 and 60 °C with ~12 °C and 70 °C as the extreme low and high mild alkaline conditions, respectively (Table 4).

Table 4 Process conditions for mild and severe alkaline treatments of wheat residues

Mild Alkaline Treatment		Severe Alkaline Treatment	
Temperature, °C	NaOH Concentration, wt.%	Time, min	NaOH Conc., wt%
40.000	1.293	30	8
40.000	2.707	30	12
40.000	2.000	90	8
40.000	2.000	90	12
40.000	2.000	60	10
40.000	2.000	60	10
40.000	2.000	60	10
60.000	1.500	60	7.17
60.000	2.500	60	12.83
20.000	1.500	17.57	10
20.000	2.500	102.43	10
68.280	2.000		
11.720	2.000		

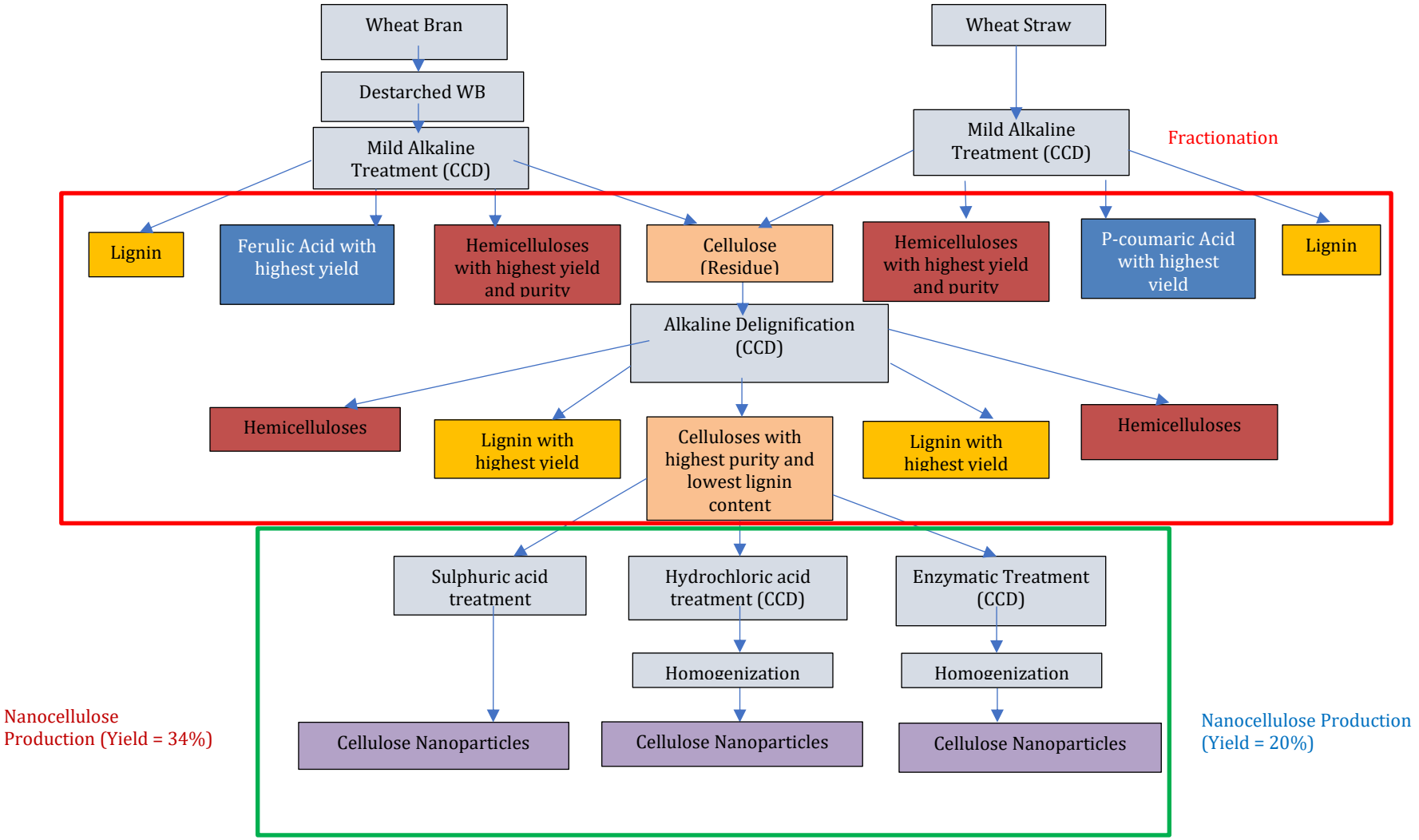

Figure 2: Fractionation routes for valorization of wheat waste into high-value products

2.1.3 Production of nanocellulose from pretreated wheat residues

2.1.3.1 *Materials and methods*

The cellulose-rich residues from the two-stage alkaline treatment (described in section 2.1.2, were treated with either hydrochloric acid (4 M HCl) at a fiber to acid ratio of 1:20 and varied time between 4 and 8 h and temperatures between 80 and 121 °C or with enzymes, Viscozyme and FiberCare at dosages that were varied at three levels 50, 75 & 100 endo-1,4-β-glucanase unit (4500 ECU)/g biomass for dosages and 10, 15 & 20 fungal β-glucanase units (100 FBG)/g biomass (Novozyme), respectively to produce nanocellulose, which were termed HCN and ECN, respectively.

The nanocelluloses extraction optimal conditions in these two processes were identified using the response surface methodology (RSM) and desirability approach in Statistica software® and were validated experimentally. The CNF production conditions were optimized in central composite design (CCD) experiments (Table 4) for yield, particle size, polydispersity index, and surface charge (Zeta Potential (ZP)) of the recovered CNF (Ceaser & Chimphango, 2021). A comparative analysis of the CNF physical (particle size, polydispersity index (pdI)), and the functional properties (ZP, thermal stability, crystallinity, and presence of functional groups) of CNF produced by the two methods was performed to ascertain their end-use applications. The commercial CNC and CNF obtained from the University of Maine were used as controls.

2.2 Project 2: Development of a process route for co-extracting nanocellulose and high value-added products from mango seed

2.2.1 Background

Mango (*Mangifera Indica L.*) is the fifth fruit in the world ranking of tropical fruits. In South Africa, about 38,300 tons of mangoes were produced in the year 2015/2016 (Ntshangase *et al*., 2016) and the production is likely to increase with time. ‘Tommy Atkins’, ‘Kent’, ‘Keitt’, ‘Zill’ and ‘Heidi’, are some common varieties grown in South Africa with Limpopo and Mpumalanga provinces as the major producers (DAFF, 2011). The mango fruit comprises the seed, the mesocarp and peels. The peel constitutes 30.0 – 45.0% of the mango fruit (Da *et al*, 2010). The seed makes up 10.0 – 25.0% of the whole fruit and contains 45.0 – 85.0% kernel (Kittiphoom, 2012; Leon, 2016). The mesocarp of mango is usually processed into different products including dried fruit pulp, frozen mango pulp and canned mango pulp (Kittiphoom, 2012; León, 2016). The mango peel and seeds are considered by-products that are discarded during mango processing (Ajila *et al.*, 2007a). These by-products account for 35.0 – 60.0% of the total weight of mango fruit (Dorta *et al*. 2012; León, 2016). The mango waste constitutes 45.0% of the global waste produced during agricultural fruit processing (Menon, Dutta, Majumdar & Ravi, 2014). Yet, these wastes contain considerable amounts of valuable products that could be explored and used in different applications (Kittiphoom, 2012).

Polyphenols and phytochemicals extracted from the mango fruit wastes have been used as antioxidants in many applications, both the food and non-food industries (Ajila *et al.*, 2007b). During the mango fruit processing, apart from the pulp, the residues containing seeds and peels accounting for 35 – 55% of the whole fruit, depending on the variety of the are disposed of as waste (Ajila *et al*. 2007a, Kittiphoom, 2016). The mango seed consists of an outer layer (husk) and an inner stone (kernel). The seed contains appreciable amounts of polyphenols, cellulose and other cell wall components, and hence, could be explored further for valorization to specialty foods and biomaterials with environmental benefits (Chinga-Carrasco, 2011; Menon *et al*., 2014). The cellulose component is a potential resource for nanocellulose production (Eichhorn *et al*., 2010) that can be used for different applications including gas barrier films, biomedical, and bioimaging (Lee *et al*., 2014a,b; Ayrilmis *et al*., 2016). An estimated volume of nanocellulose applications identified on recent market size in the USA ranges from 3.6 to 9.3 million metric tons and 0.48 million metric tons/year for applications that require high volumes and low volumes respectively (Shatkin *et al*., 2014).

The complete valorization of the mango wastes requiring co-extraction of all the components in high yields and quality has the potential to increase the value of the waste. However, the current focus has been limited to the extraction of individual components from either the seed kernel or husk (Cordeiro *et al.*, 2014; Kittiphoom, 2016; Ajila *et al*., 2007b; Tunchaiyaphum *et al*., 2013; Masibo & Qian, 2008) and the mango peel (Arora *et al.*, 2018). Thus, there is an opportunity to develop new processing methods with optimized conditions for complete valorization, using an integrated biorefinery approach (Fig 3).

The production of nanocellulose is easy to attain with feedstocks containing pure cellulose such as cotton (Table 2). The lignocellulosic materials would require the removal of the amorphous components (hemicellulose, lignin and polyphenols). However, the extraction conditions for have to be optimized for the yield and quality of the cellulose as well as the amorphous components as additional high-value products. A comprehensive fractionation process for mango waste into multiple product streams depicted in Figure 3 is the basis for an innovative integrated biorefinery, which has not yet been described in the literature and is explored in this project.

.

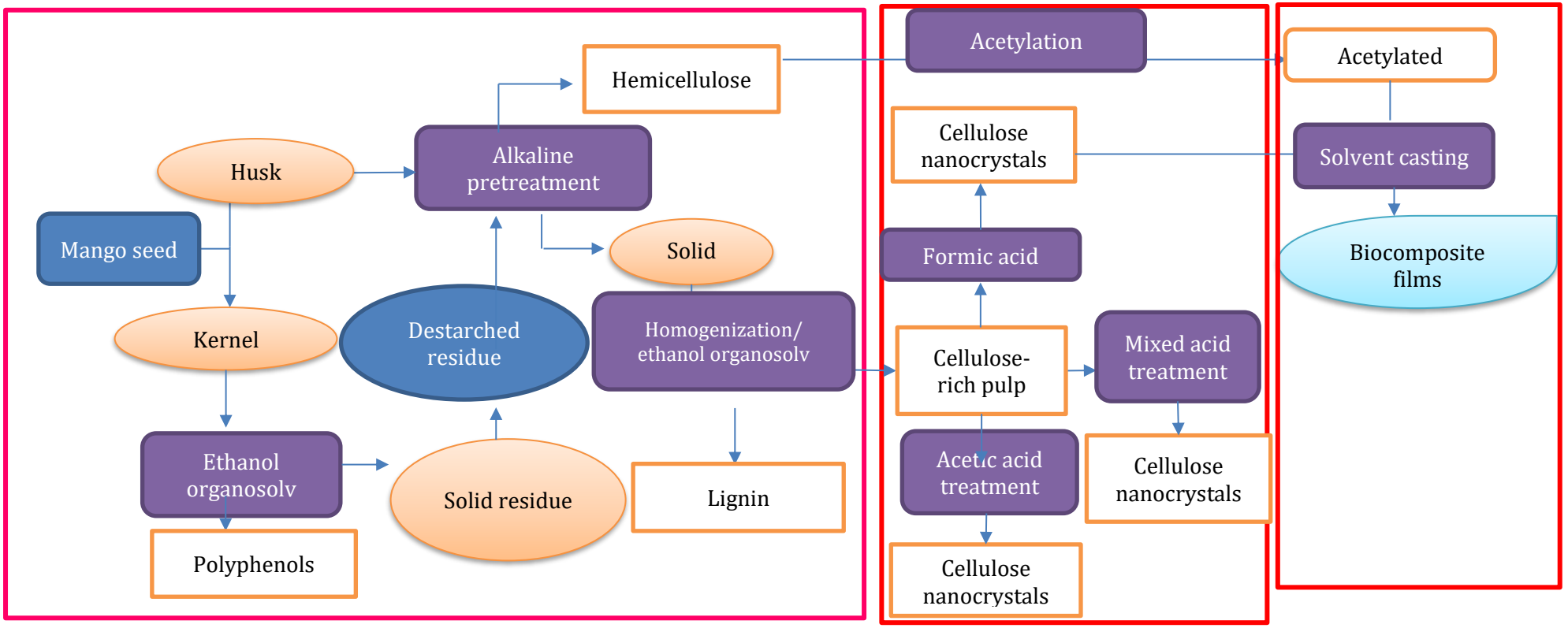

Figure 3: Fractionation routes for mango waste valorization to produce high-value products

2.2.2 Production of hemicelluloses, lignin, phenolic compounds

2.2.2.1 *Materials and methods*

Fresh ripened mango fruits (*Mangifera indica L.*) of the Kent variety were obtained from the Cape Town market in South Africa. Tommy Atkins mango seeds were obtained from Hoedspruit fruit processors (South Africa). Commercial tamarind seed xyloglucan (CXGN), beechwood xylan (CXLN), and analytical grade sugars including D-glucuronic and D-galacturonic acids were purchased from Megazyme International, Ireland. Carbazole, D-glucose, D-xylose, L-arabinose, and D-galactose were purchased from Sigma-Aldrich. All chemicals were of analytical grade. Ethanol (95%) was purchased from KIMIX, South Africa, NaOH and acetic acid (98%) were purchased from Science world, South Africa, sulphuric acid (72%), Formic acid (88 wt%), and sulphuric acid (64 wt%) were purchased from Sigma Aldrich, South Africa, dimethyl sulphoxide, dimethylacetamide, and dimethylformamide was purchased from KIMIX, South Africa. All chemicals used were of analytical grade.

Individual components from the mango waste were fractionated in a stepwise fashion. Two pretreatment/fractionation methods, thus, the mild alkaline- and organosolv-based methods (Fig 3) were applied to fractionate the mango waste in a biorefinery set-up prior to nanocellulose production. To ensure high yields and high quality of the co-products are obtained, the labile fractions such as the polyphenols from the kernel were extracted first using organosolv treatment, prior to hemicellulose extraction (Fig. 3). The mild alkaline treatment was optimized for polymeric hemicellulose extraction based on the central composite designed experiments (Table 5) while the homogenized-assisted organosolv process (Table 6) was optimized for the extraction of lignin and cellulose-rich residues from the mango husks, which constituted the raw material for nanocellulose production (Bello & Chimphango, 2021).

The effects of homogenization time on lignin dissolution from the mango seed husks were assessed at a constant temperature and ethanol concentration (150 ℃ and 60%v/v ethanol with 0.2% NaOH). The homogenization (22000 rpm) was performed with pre-soaked alkaline treated mango seed husk samples for 5, 10, 15, 20, and 30 min (Table 6) before performing optimization experiments.

Table 5 Central composite experimental design for alkaline extraction of hemicelluloses from mango-seed husks

NaOH Concentration [M]	Temperature [°C]	Time [h]
1.00	40.00	2.00
1.00	40.00	4.00
1.00	90.00	2.00
1.00	90.00	4.00
2.00	40.00	2.00
2.00	40.00	4.00
2.00	90.00	2.00
2.00	90.00	4.00
0.66	65.00	3.00
2.34	65.00	3.00
1.50	23.00	3.00
1.50	107.00	3.00
1.50	65.00	1.32
1.50	65.00	4.68
1.50	65.00	3.00
1.50	65.00	3.00
1.50	65.00	3.00
1.50	65.00	3.00
1.50	65.00	3.00
1.50	65.00	3.00

The resulting cellulose-rich residues were subjected to various acids treatments (sulphuric, acetic, and formic acids) as shown in Figure 3 to produce cellulose nanocrystals (CNCs) known as SCNC, ACNC, and FCNC, respectively, that were optimized in a central composite design (CCD) experiment as shown for formic acid treatment (Table 7).

Table 6: Central composite experimental design for organosolv extraction of lignin from alkaline treated mango seed husks

Ethanol concentration [%]	Temperature [°C]	Homogenizing time [h])
50.00	130.00	10.00
50.00	130.00	20.00
50.00	150.00	10.00
50.00	150.00	20.00
70.00	130.00	10.00
70.00	130.00	20.00
70.00	150.00	10.00
70.00	150.00	20.00
43.18	140.00	15.00
76.82	140.00	15.00
60.00	123.18	15.00
60.00	156.82	15.00
60.00	140.00	6.59
60.00	140.00	23.41
60.00	140.00	15.00
60.00	140.00	15.00

Note: Homogenization speed was 22000 rpm

2.2.3 Production of nanocelluloses from mango seed husk

Nanocellulose in the form of nanocrystals (CNCs) were produced following a modified method of Du *et al*. (2017) using formic acid hydrolysis. The experimental design is presented in Table 7. The formic acid was recovered by distillation at 100 ºC. The solids were subsequently washed several times with distilled water until pH 6 was reached. The CNCs were dialyzed using a cellulose membrane dialysis tubing with a molecular cut-off of 14000 Da (Sigma-Aldrich, USA) for 3 days against distilled water to remove the salts before freeze-drying. Acetic acid nanocelluloses (ACNC) were produced using 99.9% v/v acetic acid at varied solid-to-acid ratios (1:20 to 1:40 g/mL) for durations of 6 – 12 h in 250 mL three-neck flasks equipped with a condenser at 110 °C. The hydrolysates were centrifuged (8000 rpm) to separate the liquid and the solid fractions. The ACNCs were washed several times with distilled water until a pH 6 was reached before dialyzing using a cellulose membrane dialysis tubing (molecular cut-off of 14000 D, Sigma-Aldrich, USA) in distilled water for 3 days. The prepared nanocelluloses were freeze dried.

Table 7: Central composite experimental design for production of nanocelluloses using formic acid

Sample	Acid-to-pulp ratio mL/g	Reaction time [h]
	20	6
2	20	10
3	40	6
4	40	10
5	15.9	8
6	44.1	8
7	30	5.17
8	30	10.83
9	30	8
10	30	8

The reference CNCs were produced using unbleached and bleached mango seed husks following the sulphuric acid method (64 wt% sulphuric acids for 60 min at 60 °C) at an acid-to-pulp ratio of 30:1 mL/g. Thereafter, the SCNCs were dialyzed and dried at 40 °C overnight (Silva *et al*., 2019).

2.2.4 Production of hemicelluloses and phenolic compounds from mango seed kernel

Mango seed kernels were subjected to organosolv pretreatment involving ethanol concentrations ranging from 40 - 80%v/v, and temperatures 20 - 60 °C, for polyphenol extraction. Hemicelluloses extraction from the polyphenol extracted seed kernel residue was with 1 -.2 M NaOH at 40 - 90°C for 2 - 4h. The polyphenol extracted solid residue was destarched using thermostable α-amylase (Termamyl®SC) and amyloglucosidase (Saczyme®Plus) enzymes (from Novozymes) before extracting hemicelluloses using an alkaline method.

2.3 Characterization and quantification of raw materials and products:

The raw materials were sampled by a coning and quartering method before being milled using a Retch ZM200 equipped with a 2mm circular blade to mill to a sample size of about 250- 425µm. The milled samples were further screened in a Retch AS200 shaker to obtain samples within the specified size range for compositional analysis.

The prepared raw materials were conditioned at 25 °C for 48 h before compositional analysis, which involved the determination of sugars, polyphenols, lignin, ash, proteins and structural and physical features in terms of functional groups, crystallinity, and thermal stability. Similarly, the products were characterized at each step of the fractionation.

The sugars and phenolic compounds were characterized and quantified using high-performance liquid chromatography (HPLC). The acid sugars such as the uronic acids in the untreated biomass, and the hemicellulose extracts were measured using the carbazole-sulphuric acid method previously described by other authors (Brienzo, Siqueira, & Milagres, 2009; Chimphango *et al.*, 2012), whereas, the chemical and functional groups were identified using the Fourier Transfer Infrared Spectroscopy (FTIR) and Nuclear Magnetic Resonance Spectroscopy with cross-polarization and magic-angle spinning, CP/MAS NMR was used to obtain hemicellulose spectra on a solid-state NMR spectrometer (Varian VNMRS 500) operating at a frequency of 125 MHz, with a 6 mm T3 probe at room temperature. The morphology and particle size distributions were determined using Scanning Electron Microscopy (SEM) imaging in conjunction with image J software. Thermal stability and surface charge were determined using Thermogravimetric Analysis (TGA) and Zetasizer (Nano-ZS90 size analyzer, Malvern Instruments), respectively. Crystallinity was determined using x-ray diffraction (XRD).

2.3.1 Compositional Analysis

The compositions of raw materials and treated materials were determined by employing the National Renewable Energy Laboratory (NREL) Laboratory Analytical Procedure (LAP) methods for biomass (Sluiter *et al.*, 2012). The NREL methods were used to determine the moisture, extractives, ash, hemicellulose, lignin, and cellulose content of the biomass. The analyses were performed in triplicates.

The moisture and ash contents were quantified using Equations 1 and 2, respectively.

$$\%\ Moisture\ content = \frac{M_W - M_D}{M_D} \times 100 \quad (1)$$

Where: M_W and M_D are the initial and oven-dried mass of the sample, respectively.

$$\%\ Ash\ content = \frac{M_{AC} - M_c}{M_w} \times 100 \quad (2)$$

Where: M_{AC}, M_C and M_W are mass of ash and crucible, mass of crucible and mass of sample, respectively.

The water and ethanol extractives were determined separately but both were accounted for using Equation 3

$$\%\ Extractive\ (X) = \frac{M_{FE(X)} - M_F}{M_W} \times 100 \quad (3)$$

Where: (X), M_{FE}, M_F, M_W represents water or ethanol, mass of oven-dried flask with extractives, mass of flask and mass of sample, respectively.

The lignin was determined after performing a two-step acid hydrolysis on the extractive free samples (Sluiter *et al*., 2012)

The total lignin content was the sum of the acid-insoluble (AIL) e and acid-soluble lignin (ASL).

$$AIL = \frac{(M_{CR} - M_C) - (M_{CA} - M_C) - M_P}{M_D} \quad (4)$$

Where: AIL, M_{CR}, M_C, M_{CA}, M_P, and M_D are acid insoluble lignin, mass of crucible and oven dried hydrolysis residue, mass of crucible, mass of crucible and ash, mass of protein in sample and mass of oven-dried sample, respectively.

$$ASL = \frac{UV_{wav} \times V_f \times Dilution}{\varepsilon \times M_D} \times 100 \quad (5)$$

Where: ASL, UV_{wav}, V_f, Dilution, ε and M_D are acid-soluble lignin, sample absorbance at 240 nm, volume of filtrate, biomass absorptivity (25 L/gcm) and mass of oven dried sample, respectively

The hemicelluloses and cellulose contents were determined and characterized using HPLC, which had an Aminex HPX-87H ion exclusion column with a 65 °C column temperature and a flowrate of 0.6 mL/min. The HPLC system also had Shodex R 101 refractive index which was operated at 45ºC. The HPLC showed the presence of xylose, arabinose, cellulose, furfural and 5-hydroxymethylfurfural (HMF)). The hemicelluloses were a combination of the xylose and arabinose content (Equation 6), whereas the cellulose (glucan) was determined based on glucose content (Equation 7) of the samples.

$$Hemicellulose\ content = 0.88 \times (arabinose + xylose) \quad (6)$$

$$Cellulose\ content = 0.9 \times (glucose\ content) \quad (7)$$

The mango seed husks composition was determined based on the acid detergent fibre (ADF), neutral detergent fibre (NDF), and acid detergent lignin (ADL) to account for the content of cellulose, hemicellulose, lignin, and other components according to the Van Soest method using Fibertech®

system (Velp Scientifica 419278, FIWE, raw fibre extractor). Equations 8, 9, and10 accounted for the percentage of hemicelluloses, cellulose, and lignin in the material, respectively.

$$Hemicellulose\ (\%) = \frac{m_{NDF} - m_{ADF}}{m_{sample}} \times 100 \quad (8)$$

$$Cellulose\ (\%) = \frac{m_{ADF} - m_{ADL}}{m_{sample}} \times 100 \quad (9)$$

$$Lignin\ (\%) = \frac{m_{ADL} - m_{crucible}}{m_{sample}} \times 100 \quad (10)$$

The presence of xyloglucan was determined through glycosidic linkage analysis using a method of Ciacanu & Kerek (1984) that is based on methylation of polysaccharides in addition to FTIR and NMR. The acetylated derivatives were extracted with 2 mL of dichloromethane and analyzed by gas chromatography (Agilent, 6890 N, Palo Alto, CA), coupled with an Agilent mass spectrometer detector (Agilent 5975 MS, Palo Alto, CA). The GC-MS system was equipped with a non-polar guardian (30 m; 0.25 mm; 0.25 µm film thickness) ZB 7HG-G027-11 GC capillary column. Helium was used as carrier gas with a flow of 1 mL/min. The injector temperature was maintained at 250 ºC and the oven temperature was as follows: 80ºC for 1 min; and finally ramped up to 300 ºC at 7 ºC min^{-1} and held for 2 min. The MSD was operated in full scan mode and the source and quad were maintained at 240 ºC and 150 ºC, respectively. The scan rate was between 40-600 m/z.

The crude protein and starch contents of the samples were estimated from the Kjeldahl method using a nitrogen factor of 6.25 (Hames *et al*., 2008) and by use of a starch assay kit (KSTA 09/14) from Megazyme. The protein content was determined by the equation 11:

$$Protein\ content = \frac{(V_{ts} - V_b) \times 1.4007 \times 0.2 \times 6.25}{M_D} \quad (11)$$

Where: V_{ts}, V_b and M_D are volume of titrated sample, volume of titrated blank, and oven dried mass of sample (1.0 g), respectively.

2.3.2 Bioproduct yield and functional properties

The polyphenols the from mango seed kernel were determined based on the total polyphenols following the Folin-Ciocalteau method (Dorta, Lobo & Gonzalez, 2012) and antioxidant activity by DPPH free radical scavenging activity. The DPPH free radical scavenging activity of *ferulic* acid (from wheat bran) and *p*-Coumaric acid (from wheat straw) was determined by using the method described by Phongthai *et al*. (2016). A 0.25 mL aliquot of the sample (*ferulic* or *p*-coumaric acid) was mixed with 1 mL of 0.1 mM DPPH in 95% ethanol. The absorbance of the various mixtures was determined by using a spectrophotometer (Cecil CE 2021, 2000 Series, (Lasec SA (Pty Ltd)) at 517

nm against the blank. The scavenging activity for DPPH (S) was determined by using the equation (12)

$$\%S = \frac{Absorbance_{blank} - Absorbance_{sample}}{Absorbance_{blank}} \times 100 \quad (12)$$

The yields of all CNCs prepared were determined gravimetrically according to Equation 13.

$$Yield\ (\%) = \frac{mass\ of\ freeze-dried\ sample\ (g)}{mass\ of\ starting\ material\ (g)} \times 100\% \quad (13)$$

2.3.3 Structural and physical properties

The structural and physical properties of the raw materials and the products were analyzed by FTIR, TGA, SEM, Zetasizer, and XRD.

2.3.3.1 ***Fourier Transfer Infrared Spectroscopy (FTIR) and Nuclear Magnetic Resonance (NMR)***

Functional groups and any chemical and structural changes of the raw materials and bioproducts were determined using FTIR and NMR. The FTIR analysis was performed in the wavelength range of 400 – 4000 cm^{-1} with a resolution of 4 cm^{-1} using a Thermo Nicolet Nexus 670 spectrometer. This was conducted by powdering dried samples into ultra-thin pellets and measured with the attenuated total reflectance mode of the spectrometer of which 32 scans were taken. The peaks of the spectra obtained were assigned according to literature (Kumar *et al*., 2014); Warren *et al*., 2015. Hou *et al.*, 2017; Zheng *et al.*, 2018) . The functional groups, in particular, for the hemicelluloses, were identified using solid-state NMR spectrometer (Nuclear Magnetic Resonance Spectroscopy with cross-polarization and magic-angle spinning, CP/MAS NMR (Varian VNMRS 500) operating at a frequency of 125 MHz, with a 6 mm T3 probe at room temperature).

2.3.3.2 ***Acetyl groups determination***

Acetyl content and degree of acetylation for the ACNCs were determined using Equation 14.

$$Acetyl\ content(\%) = [(B - A)N_a + (C - D)N_b] \times \left(\frac{4.035}{W}\right) \quad (14)$$

Where: A is the volume of A added to the sample (mL), B is the volume of A added to the blank (mL), C is the volume of NaOH added to the sample (mL), D is the volume of NaOH added to the blank (mL), W is the weight of the sample (g), and Nc and Nd are the normality of the HCl and NaOH solutions, respectively. The average number of acetyl groups per anhydro-D-glucose unit of cellulose (DS) could be calculated from Equation 15:

$$DS = \frac{3.86 \times Acetyl\ content(\%)}{102.4 - Acetyl\ content(\%)} \quad (15)$$

Where: DS is the degree of acetyl substitution.

2.3.3.3 *Molecular weight*

The molecular weights (Mw) were determined by gel permeation chromatography (GPC) using HPLC. HPLC (Dionex Ultimate 3000 system with ELS detection equipped with a 3 x 300 mm PSS SUPREMA column set) analysis. Ammonium acetate concentration of 0.125 M was used as the eluent at a temperature of 75 °C and a flow rate of 1 mL/min. Pullulan was used as a molecular weight standard.

2.3.3.4 *X-Ray Diffraction and Crystallinity*

The Crystallinity Index (CI) was determined based on X-ray diffraction using a Bruker D2 Phaser x-ray diffractometer with a monochromatic CuKα radiation source (λ=1.54184 Å, 30 kV) with a 2θ angle range from 5° to 50° (1°/min) at room temperature. Each coin-sized sample was grounded into powder and leveled on a sample holder to promote uniform and complete exposure to the x-ray (Johar *et al*., 2012). The CrI was calculated using the Segal method (Equation 16) (Rosa *et al*., 2012). This involved using the height of 2 0 0 peak ($I_{2\,0\,0}$, 2θ = 22.5°) and the minimum between the 2 0 0 and 1 1 0 peaks (I_{am}, 2θ = 18°) for the calculation:

$$CrI = \frac{I_{2\,0\,0} - I_{am}}{I_{2\,0\,0}} \times 100\% \qquad (16)$$

2.3.3.5 *Scanning Electron Microscopy*

Fiber morphology and biocomposite structures were characterized using scanning electron microscopy (SEM). The SEM micrographs of the treated fibers were taken in quadruplets using a MERLIN, Zeiss scanning electron microscope operated at 3 kV and higher, in which the fiber samples were coated with gold to eliminate the electron charging effects . The morphological changes of the fractionated fibers were observed from micrographs obtained, however for the produced nanocelluloses additional information of the fiber length and diameter were determined by using image j software in conjunction with the micrographs. On average, 50 measurements were taken for each image for the four SEM images for the nanocelluloses of which an average was estimated and used as the sample length and diameter.

2.3.3.6 *Thermogravimetric Analysis (TGA)*

The thermal stability of the materials was determined using a Mettler Toledo TGA, Thermogravimetric analyser (TGA500) with a heating rate of 10 °C/min within a temperature range of 25 – 600 °C in a nitrogen atmosphere to prevent any thermoxidative degradation (Moran *et al*., 2008). The analysis was done to compare the thermal degradation of the treated fibers with the untreated ones, to determine the effects of the treatment on the products.

2.3.3.7 *Particle Morphology and Surface Charge Analysis*

The morphological and surface charge properties of the materials in the form of particle size, polydispersity index (PdI) and Zeta potential (ZP) were determined using a Zetasizer (Nano-ZS90 size analyser (Malvern Instruments)). The analysis was based on a dynamic light scattering method after a dilution of the sample to less than 0.01% (w/w). Analysis by the equipment occurred after 120 s equilibrating time at a scattering angle of 90° at 25 °C. The measurements were taken in triplicate and the intensity-weighted mean hydrodynamic diameter was calculated by the instrument by using a cumulative method. This resulted in obtaining a mean particle size with most of the intensity peak.

2.3.4 Statistical analysis

The experimental designs were based on the central composite designs (CCD) as presented in Statistica software (TIBICO Software Incorporation, version 13.2). The statistical analyses included analysis of variance (ANOVA), desirability, and regression. The ANOVA function was used to determine the significance of the independent variables to the responses obtained at (p<0.05), as well as how well the experimental responses correlated with the predicted responses by the model. The ANOVA analysis was also used to determine if the treatment conditions (independent variables) were able to reach the optimum treatment condition for the various responses which was referred to as a quadratic term. Similarly, the ANOVA analysis determined if the responses directly increased or decreased with the increase in the independent variable referred to as the linear term.

Response surfaces and predictive models were generated for the response surfaces based on the response surface methodology (RSM) using the Statistica software®. In addition, the desirability function was used to generate desirability plots and optimized conditions for the independent variables with respect to the responses from the experiment. Means and standard deviations for measurements were determined from replicate measurements generated in either Statistica Software® or Microsoft Excel, 2013.

3 Results

3.1 Two Stage-Alkaline Treatment of Wheat Straw and Wheat Bran

The wheat bran and wheat straw had compositions (Table 8) that were similar to the compositions reported in literature (Table 2). Wheat straw was rich in cellulose while wheat bran (undestarched) was rich in starch ~30% and hemicelluloses (~34%) when destarched (Table 8).

Table 8 Chemical composition of untreated wheat straw, untreated wheat bran and destarched wheat bran.

Composition	Untreated Wheat Straw	Untreated Wheat Bran	Destarched Wheat Bran
Cellulose, %	35.7 ± 2.4	10.3 ± 0.6	16.7 ± 0.4
Hemicelluloses, %	18.8 ± 1.4	22.0 ± 0.8	33.7 ± 0.7
Lignin, %	19.3 ± 3.2	11.2 ± 0.5	18.6 ± 0.7
Starch, %	3.9 ± 0.2	30.0 ± 0.3	0.4 ± 0.2
Protein, %	1.3 ± 0.3	14.9 ± 2.5	15.4 ± 4.8
Ash, %	3.6 ± 0.1	3.7 ± 0.1	2.4 ± 0.2
Extractives, %	13.9 ± 0.4	9.8 ± 0.8	8.4 ± 0.5
Ferulic Acid, %	0.17 ± 0.04	0.28 ± 0.05	0.34 ± 0.03
p-Coumaric Acid, %	0.24 ± 0.03	-	0.07 ± 0.01
Total, %	**96.8**	**102.2**	**100.8**

The mild alkaline stage in the two-stage fractionation method enabled the production of hemicellulose, lignin and hydroxycinnamic acids (*ferulic* from wheat bran and *p*-coumaric acid from wheat straw), and cellulose-rich residues with desirable attributes for industrial applications. The optimal conditions for the mild alkaline conditions were between 50 and 60 ºC and between 2.0- 3.0 wt% NaOH for wheat straw and about 70 ºC and 2-3 wt. % NaOH for the wheat bran.

The severe alkaline stage in the two-stage alkaline treatment permitted the recovery of cellulose. However, increasing these treatment conditions beyond the 10 wt. % NaOH and 60 min resulted in a decrease in the cellulose yield for wheat straw. In wheat bran, the highest cellulose recovery was with a NaOH concentration of 8 wt.% and reaction time of 60 (Table 9).

The total yield for hemicelluloses and lignin after the two-stage alkaline treatment ranged between 65 and 80% from the wheat straw. In addition, a *p*-coumaric yield above 80% with an antioxidant activity >40% was obtained (Table 9). The cellulose recovery from the wheat straw cellulose residues was >90% with a cellulose content >70%. The cellulose-rich residue crystallinity >50% rendered the residues suitable for nanocellulose production. On the other hand, wheat bran was rich in hemicellulose (> 50%) and lignin (>90%) with *ferulic* acid >60% (Table 9). The cellulosic residue recovery for the wheat bran was over 80% but contained < 50% cellulose with over 30% and 5% residual hemicellulose and lignin, respectively (Table 9).

Table 9 Yield and quality of fractionated products at optimal conditions for the mild alkaline treatment of wheat straw and wheat bran for hemicellulose

Optimized Mild Alkaline Conditions Wheat Straw (~55ºC, 2.4 wt.% NaOH)			
	Hemicelluloses Purity, %	Actual Hemicelluloses Yield/Raw WS Hemicelluloses, %	*p*-Coumaric Acid Yield, %
Predicted Values	38.68 ± 1.29	34.60 ± 0.49	84.80 ± 2.04
Experimental Values	37.85 ± 0.19	34.73 ± 0.31	85.29 ± 2.84

Optimized Mild Alkaline Conditions Wheat Bran (68 ºC, 2.7 wt.% NaOH)			
	Hemicelluloses Purity, %	Actual Hemicelluloses Yield/Raw WB Hemicelluloses, %	Ferulic Acid, Yield, %
Predicted Values	47.78 ± 3.51	33.67 ±7.27	64.32 ± 3.5
Experimental Values	47.56 ± 0.30	36.98 ± 1.18	65.63 ± 1.0

Optimized Severe Alkaline Conditions Wheat Straw (60 min, 10 wt.% NaOH)			
	Residue Cellulose, %	Residue Lignin, %	Lignin Extracted Yield/ Original MA WS Lignin, %
Predicted Values	77.46 ± 3.71	4.95 ± 1.12	62.78 ± 3.04
Experimental Values	76.25 ± 0.66	5.17 ± 0.16	60.12 ± 1.09

Optimized Severe Alkaline Conditions Wheat Bran (81.2 min, 9.41 wt% NaOH)			
	Residue Cellulose, %	Residue Lignin, %	Lignin Extracted Yield/ Original MA WB Lignin, %
Predicted Values	47.10 ± 2.26	6.47 ± 0.23	62.35 ± 4.25
Experimental Values	48.10 ± 0.04	6.29 ± 0.86	61.51 ± 3.28

After removing the hemicelluloses, lignin, and other components, the crystallinity of the materials at each step prior to nanocelluloses production, increased to up to 41% and 55% for the wheat bran and wheat straw, respectively (Table 10). The thermal properties of the hemicelluloses and lignin extracted from the two-stage alkaline process are presented in Figures 4a and b, respectively, for hemicelluloses from wheat bran and wheat straw. The onset and maximum

decomposition temperatures (T_{onset} and T_{max}, respectively) for MAWS hemicelluloses were about 22 °C less than those of the MAWB hemicelluloses (Fig 4).

Table 10 Crystallinity of solid residues at various stages of the two-stage alkaline treatment of wheat straw and bran

Sample	Crystallinity Index, %
Untreated Wheat Bran	-
Destarched Wheat Bran	17
Mild Alkaline Treated Wheat Bran (MAWB)	34
Alkaline Delignified Treated Wheat Bran (SAWB)	41
Untreated Wheat Straw	44
Mild Alkaline Treated Wheat Straw (MAWS)	50
Alkaline Delignified Treated Wheat Straw (SAWS)	55

In case of lignin, the second weight loss began at T_{onset} of 171 °C and 147 °C for MAWS lignin and MAWB lignin, respectively (Fig. 4b). In comparison with the hemicellulose (Fig 4a), a faster oxidisation of the lignin is evident resulting in a T_{max} of 276 °C and 295 °C for MAWB lignin and MAWS lignin, respectively. The reduced T_{max} for MAWB lignin could be attributed to the larger hemicelluloses content of MAWB lignin (15.8%) than that of MAWS lignin (4.9%) . Moreover, the higher lignin content of MAWS lignin (84.4%) resulted in a higher T_{comp} (448ºC) in comparison with the 338 °C obtained by MAWB lignin with a lower lignin content (58.9%) (Fig. 4b). Consequently, charring occurred at 600 °C double that of hemicelluloses from MAWS and MAWB. The char obtained for MAWS and MAWB lignin are 49% and 29%, respectively which were similar to the lignin char obtained by other researchers ((Wild, Huijgen & Heeres, 2012; Watkins *et al.*, 2015). Therefore, there is potential to use the lignin from both MAWS and MAWB, in polymer composite materials.

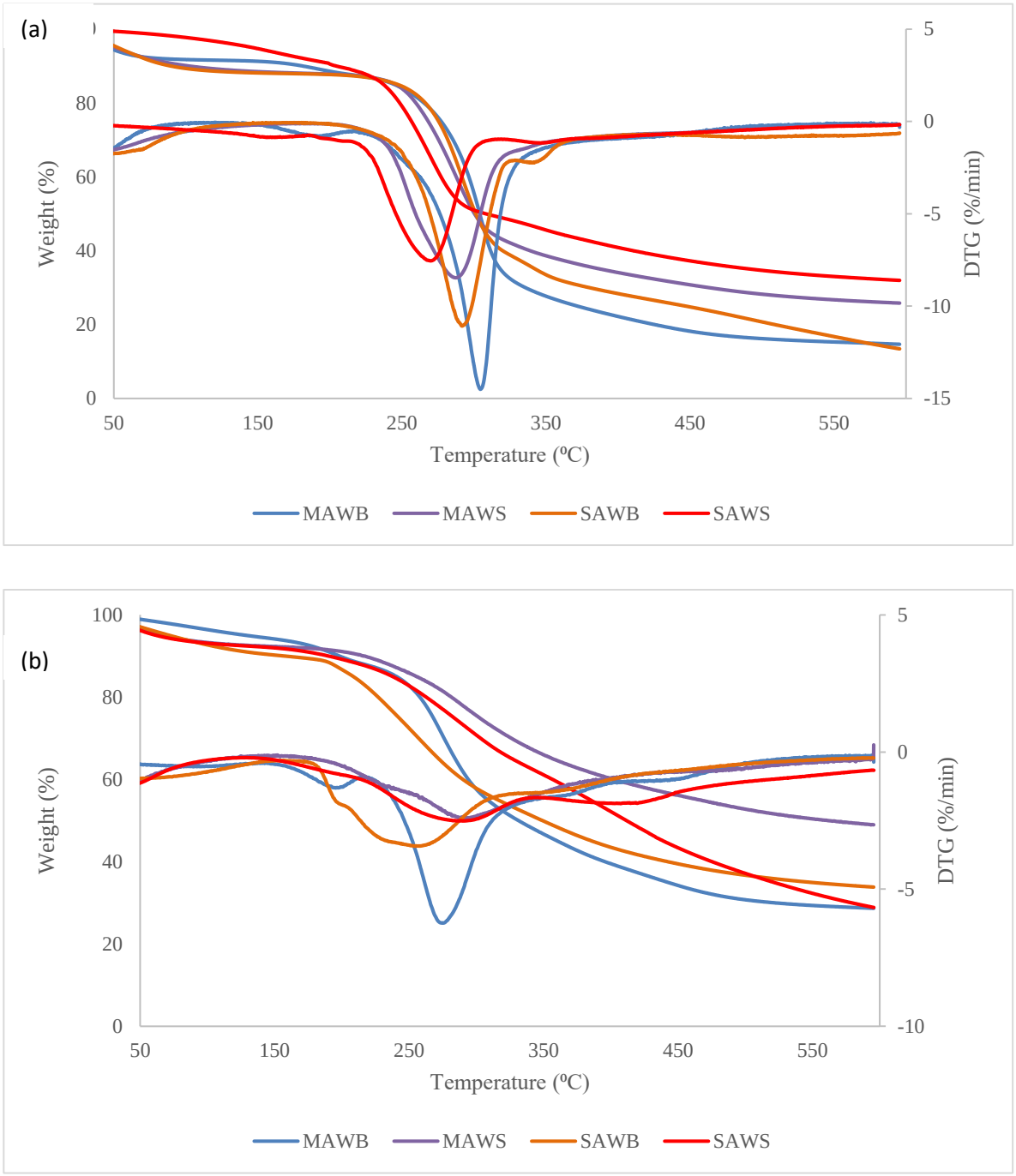

Figure 4 Thermal stability of (a) hemicellulose and (b) lignin extracted at the mild alkaline (MA) and severe alkaline (SA) stage from wheat straw (WS) and wheat bran (WB).

3.2 Nanocellulose production using hydrochloric and enzymatic Treatment of Wheat Straw and Wheat Bran

The optimal conditions for HCN production were 7.41 h, 114.14 ºC whereas, those of the enzymatic method were 4.64 h, 75 ECU/g Fibercare R dosage, and 10.80 FBG/g Viscozyme L dosage at 50 ºC (Table 11). Both the HCN and ECN yields were similar ~20% (Ceaser & Chimphango, 2021). However, the ECN was quicker to produce than the HCN for the same yield (4.64 h vs 7.41 h) and at a reduced temperature (50 ºC vs 114 ºC).

Table 11 Physical and functional properties of cellulose nanofibres produced by hydrochloric and enzymatic hydrolysis compared to commercial cellulose nanofibers (Ceaser & Chimphango, 2021)

Sample	Length, (nm)	Diameter, (nm)	Polydispersity index	Zeta potential, (Mv)	Yield (%)	CrI (%)
HCN	514 ± 50	17 ± 3	0.53 ± 0.20	-16.3 ± 1.50	20.31 ± 1.24	70
ECN	2293 ± 173	17 ± 2	0.92 ± 0.13	-15.2 ± 0.6	17.16 ± 2.30	48
Commercial CNF[a]	1824 ± 154	27 ± 8	1 ± 0.03	-14.5 ± 1	-	56

Note: CNF: Cellulose nanofibres; ECN: enzymatically produced cellulose nanofibres at (4.64 h), FibreCare Dosage (75 ECU/g) and Viscozyme Dosage (10.8 FBG/g); HCN: Hydrochloric acid produced nanofibre at optimal conditions (114.14 ºC and time of 7.41 h); CrI: Crystallinity Index and [a] reference cellulose nanofibres

The Zeta potential and maximum thermal decomposition temperature (Table 11) for the ECN (-15.2 ± 0.6 mV and 378 °C, respectively) were similar to that of HCN (-16.3 ± 1.50 mV and 380 °C, respectively). However, the HCN crystallinity (70%) was closer to that of sulphuric acid nanoparticles (75%) but higher than ECN crystallinity (48%). The HCN PdI (0.53) and fiber length (514 nm) were relatively lower than ECN's (0.92 ± 0.13 PdI and >1 µm length). Thus, Both the HCN & ECN can be classified as thermally stable nanohydrocolloids. Figure 5 depicts the morphologies of the HCN and ECN (network-like) in Figures 5b and c, compared to nanocellulose produced by the sulphuric acid method (rod-like) in Figure 5a. The HCL and enzymatic CNF production methods have shown potential synergetic effects on CNF production, morphological, and functional properties warranting further investigation.

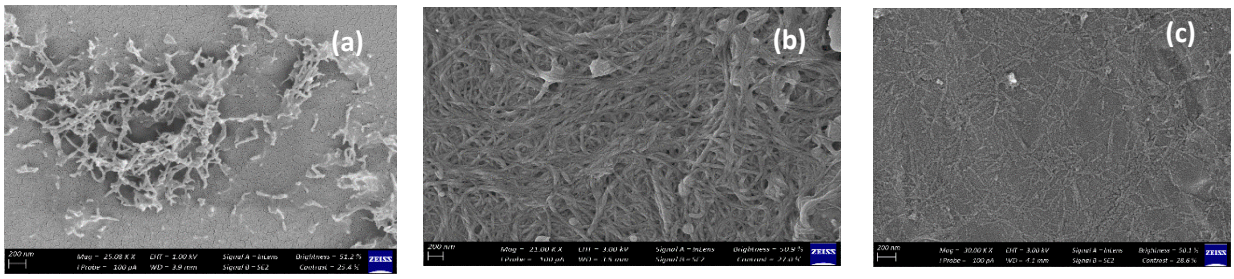

Figure 5 the scanning electron microscopy micrographs for nanocellulose produced using (a) sulphuric acid, (b) hydrochloric acid, and (c) enzymes at optimal conditions.

3.3 Development of a process route for co-extracting nanocellulose and high-value-added products from mango waste

The mango peels were rich in polyphenols (Mugwagwa & Chimphango, 2019) and contained ~15% pectin and only 26% cellulose whereas the kernel had up to 3% cellulose and 17 % hemicelluloses with lignin less than in the peels, ~4% vs ~20% respectively (Table 12)

Table 12 Compositional analysis of mango peel and kernel

Sample	Extractives%	Ash%	Cellulose%	Hemicellulose%	Lignin%	Starch (%)	Pectin/g
Mango peel	45.59	4.0	26.16	10.16	18.06	N/A	14.67
Mango Kernel	24.33	2.74	3.08	17.58	4.17	33.81	N/A
FD Peel	54.44	3.55	24.57	10.31	20.06	N/A	14.30
OD Peel	45.96	3.69	23.97	10.13	18.98	N/A	12.25
AD Peel	45.36	3.38	21.02	10.43	19.97	N/A	14.67

FD = Freeze-dried, OD = Oven - dried, AD= Air - dried

The husks had cellulose content > 50% and comparable hemicellulose and lignin contents to those found in the literature (Dzigbor & Chimphango, 2019; Torres-León *et al.*, 2019). During the mild alkaline treatment, it was evident that the lignin and cellulose contents increased (14 to 19% and 50 to 57%, respectively) with the alkaline treatment (Table 13).

Table 13 Composition of untreated and alkaline treated mango seed husk

Component	Untreated mango husks (%)	Alkaline-treated mango husks (%)
Cellulose	50.27 ± 0.35	57.08 ± 0.10
Hemicellulose	17.98 ± 0.42	9.43 ± 0.67
Lignin	14.77 ± 1.20	19.13 ± 1.09
Extractives	12.19 ± 0.61	10.50 ± 0.13
Ash	0.80 ± 0.06	0.27 ± 0.21
Others	3.99 ± 0.02	3.59 ± 0.42

[a] Values are presented in percentages based on the dry weight.

3.3.1 Production of hemicelluloses and polyphenols from mango waste

Hemicellulose yields of approximately 50% were achieved. The hemicelluloses were substituted with uronic acids (Table 14) and were co-extracted with some lignin (Table 14). The optimized conditions were NaOH concentration= 1.92 M Temperature = 86.0 ºC and Time = 3.84 that yielded suitable XGN/XLN ratio for thermal stable biocomposites. The validated optimal conditions showed that the observed component levels were close to the predicted values (Table 14).

Table 14: Hemicellulose yield and composition at optimized extraction conditions

Responses	Predicted value %	[a] Observed value %
Yield	45.71	46.24
Xyloglucan/Xylan	0.125	0.130
Lignin content	18.79	16.73
Uronic acid	15.08	12.02

[a] . Optimized extraction conditions were NaOH concentration= 1.92 M Temperature = 86.0 °C and Time = 3.84

3.3.2 Lignin production

Pure lignin ~ 80% in yield was solubilized with >90% purity at ~148 ºC and 60% ethanol with 15 min homogenization at 22 000 rpm (Table 15).The results from the desirability analysis (Statistica 13.2 software) showed that ethanol concentration of 60%, and temperature ~156 ºC with 15 min homogenization likewise, gave the maximum cellulose content and minimum lignin contents in the solid residue (Table 15).

Table 15 Predicted and observed values of responses for optimum high shear homogenization-organosolv process conditions (Bello & Chimphango, 2021)

Component	Solubilized lignin [%]	Lignin purity [%]	Cellulose content of solid residue [%]	Hemicellulose content of solid residue [%]
Predicted values	67.18	96.67	75.21	11.13
[a]Optimal conditions	70.43	96.18	77.84	10.98
No homogenization	68.58	94.74	76.75	10.16

[a] mean of triplicates determination. The optimum conditions were Ethanol concentration = 60%, Temperature = 148.41 °C and Homogenizing time = 15 min

Validation experiments confirmed the findings (Table 15). The solubilized lignin yield and its purity were comparable to that of performed at an elevated temperature of 200 ºC when non-assisted (~69% and ~95%, respectively). The solid residue from the process contained cellulose and hemicellulose contents of ~78% and 11%, respectively (Table 15).

3.3.3 Nanocellulose production

The solid residues subjected to the acid treatment, in this case formic acid, for nanocellulose production, gave a yield > 50% compared to yields (~ 38%) obtained by the sulphuric acid method (Table 16) at the optimum levels. However, the crystallinity index was higher for the SCNC 69% vs ~67 for FCNC (Table 16)

Table 16 Predicted versus observed values of formic acid nanocellulose at optimum conditions and commercial cellulose nanocrystals

Nanocellulose Component	Yield [%]	Average particle size [nm]	CrI [%]	Formate content
Predicted	65.19	25.00	67.72	0.94
Formic acid	63.99	24.13	66.40	0.92
Suphuric acid	38.34	22.50	69.02	-

Crl= crystallinity index

The morphology of the raw materials and the nanocelluloses generated using acid methods are compared in Fig 6. The raw materials consisted of the untreated (Fig. 6a) and alkali-organosolv treated husks and (Fig. 6b). The nanocellulose produced using the formic acid (FCNC) (Figs. 6b & d) (SCNC) (Figs. 6c &e), and the acetic acid (ACNC) (Fig. 6f) were spherical in shape.

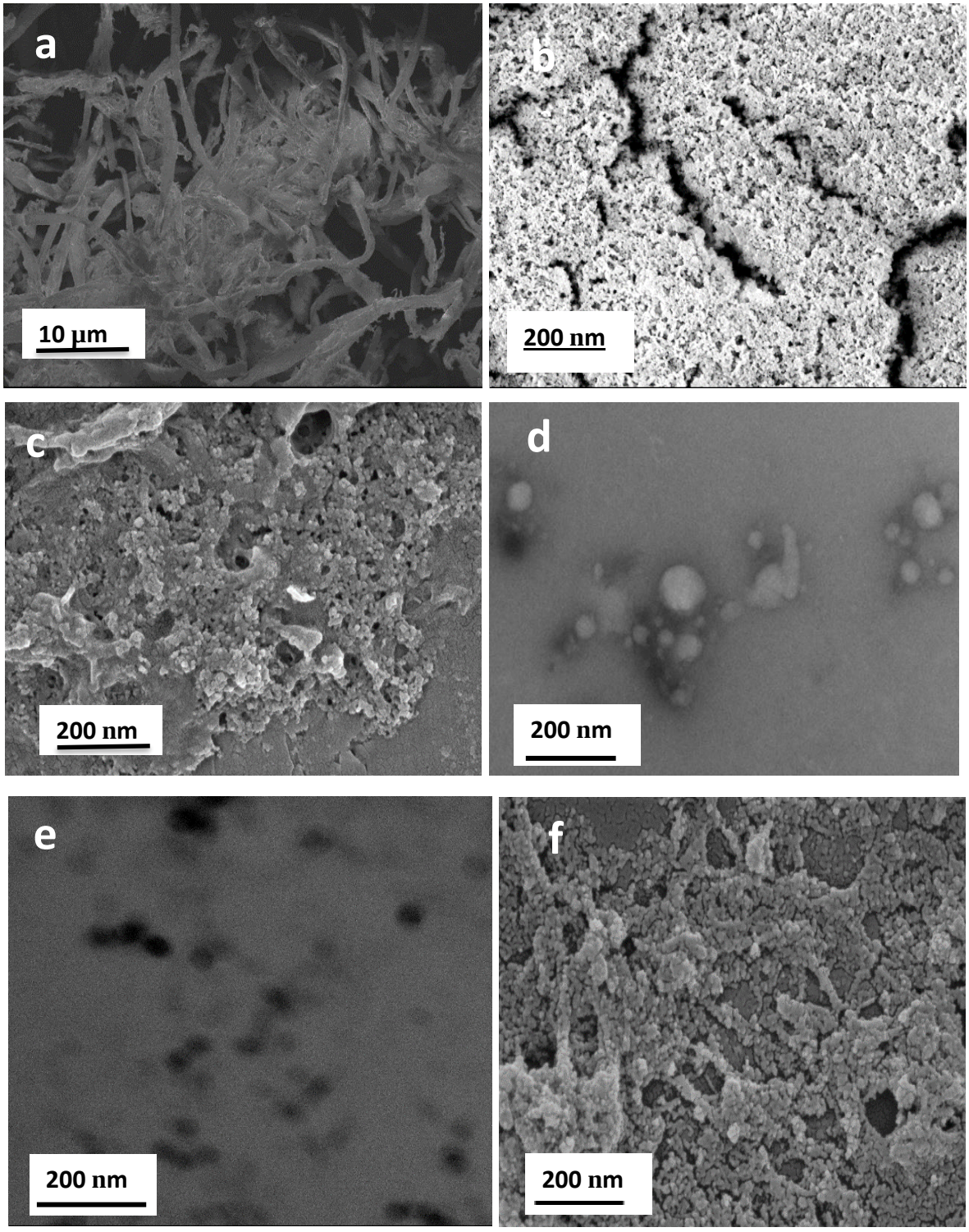

Figure 6 Scanning Electron Microscopy images of (a) unbleached pulp (b) Formic acid nanocrystals (FCNC); and (c) sulphuric acid nanocellulose. Scanning Transmission Electron Microscopy of FCNC (d) formic acid nanocellulose and (e) sulphuric acid nanocellulose and (f) Scanning Electron Microscopy images of acetic acid nanocellulose (ACNC)

The FCNC dispersed well in water, dimethylformamide (DMF), dimethylacetamide (DMAC), and dimethyl sulphoxide (DMSO), and was stable after 15 min of sonication except when in the water where aggregation was evident after 24 h at room temperature (Fig. 7).

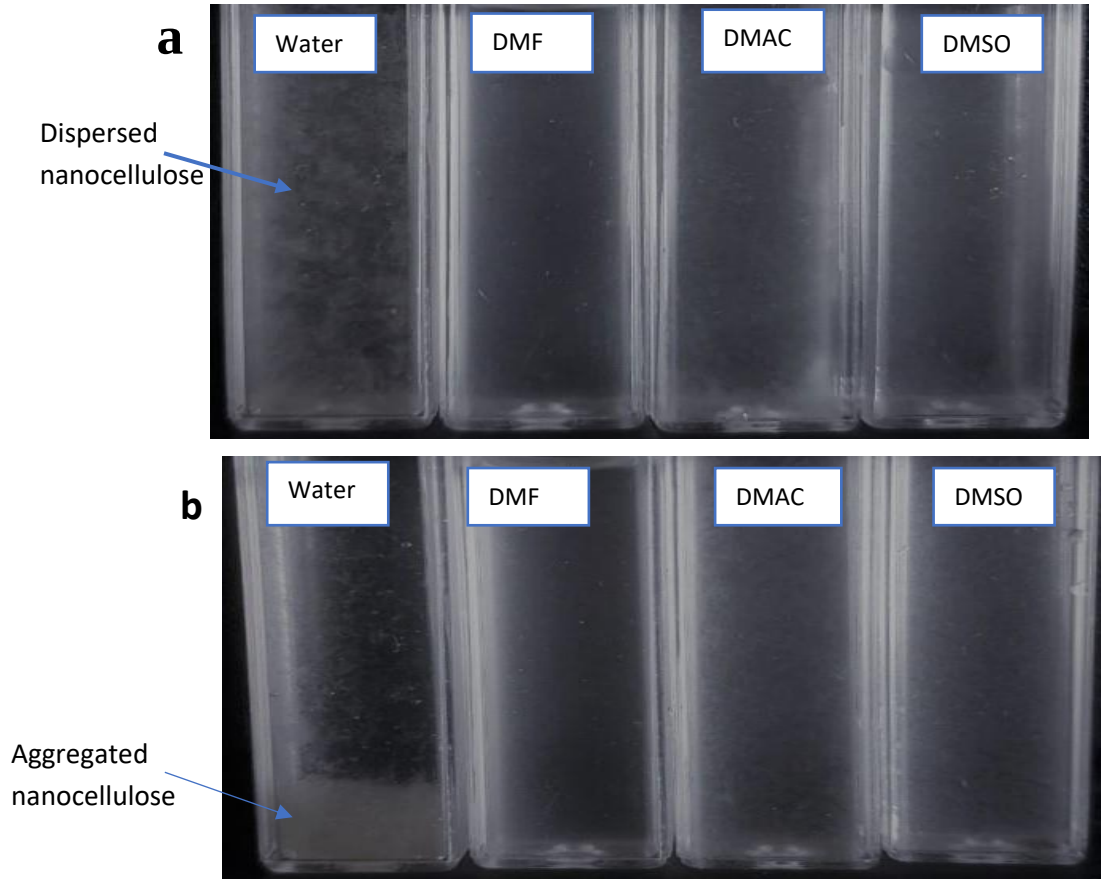

Figure 7 Images of formic acid cellulose nanocrystals dispersion in water, dimethylformamide (DMF), dimethylacetamide (DMAC), and dimethyl sulfoxide (DMSO) taken immediately after (a) sonication at 25 ºC (b) after standing for 24 h at 25 ºC

3.3.4 Formation of biocomposites

Biocomposite films formulated using commercial tamarind seed xyloglucan, commercial beechwood xylan, and extracted hemicellulose from mango seed husk formed films with different physical and surface properties. The commercial xyloglucan formed self-supporting films (Fig. 8a) while xylan, on the other hand, formed non-coherent and brittle films (Fig. 8b). Further, a combination of xyloglucan and xylan (xyloglucan/xylan ratio = 0.47) resulted in a composite film with fewer cracks, however, the film was brittle (Fig. 8c). The cracks disappeared upon the addition of 20% glycerol (Fig.8 d). The hemicellulose extracted from the mango seed husk on other hand formed self-supporting films without the addition of a plasticizer (Fig. e). The films were, however, brittle, and therefore plasticizer was added to improve the flexibility (Fig. 8f). The effect of the plasticizers and addition of FCNC on the biocomposite mechanical functional properties are presented in Figures 9 and 10, respectively.

3.3.5 Production of mango seed husk hemicellulose suitable for self-supporting biocomposite films

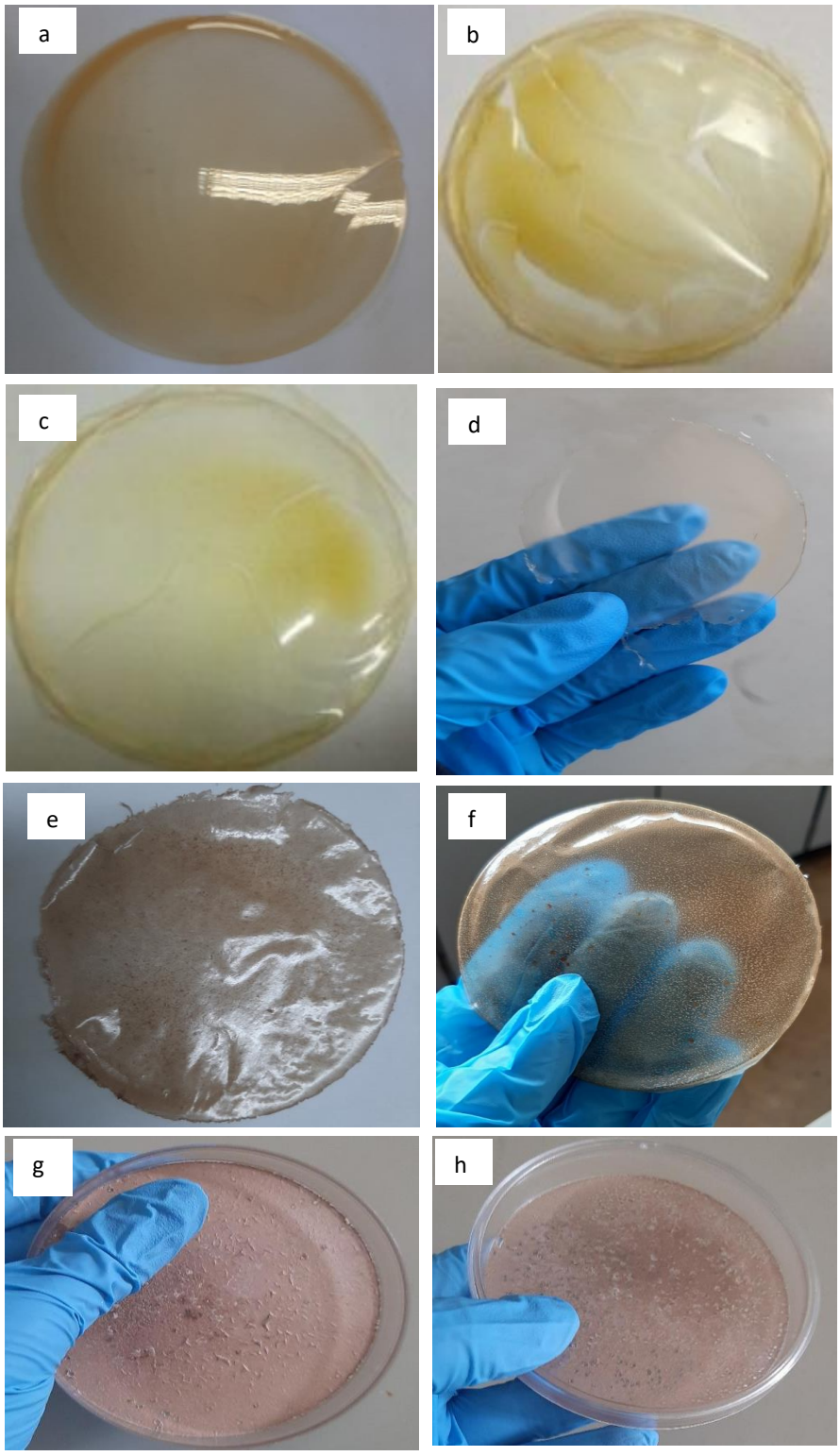

Figure 8. Biocomposite films from (a) xyloglucan, (b) xylan, (c). combination of xyloglucan and xylan (without plasticizer), (d), combination of xyloglucan and xylan (with plasticizer), (e) mango seed husk hemicellulose (without plasticizer), and (f) mango seed husk hemicelluloses with plasticizer, (g) Mango seed husk hemicelluloses with 10% and (h) 40% formic acid generated nanocellulose

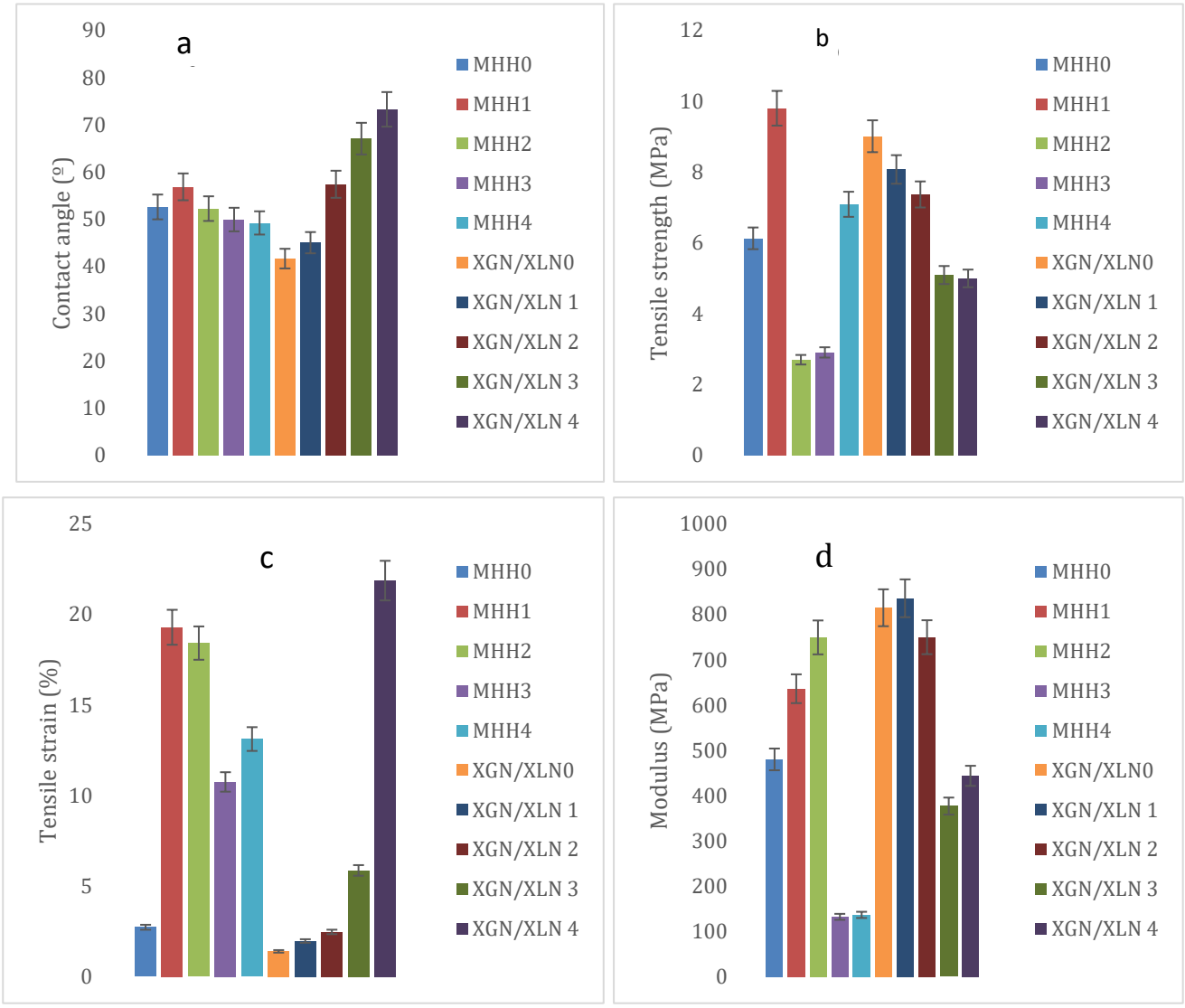

Figure 9: Effect of plasticizer content on (a) Contact angle, (b) Tensile stress, (c) Tensile strain, and (d) Modulus of mango seed husk hemicellulose and commercial hemicelluloses (xyloglucan and xylan): MHH=mango seed husk hemicellulose, XGN/XLN = xyloglucan/xylan ratio, with 0, 10, 20, 30 and 40% plasticizer.

The water contact angles for the MHH films with and without plasticiser were within 50-60º whereas those with pure xyloglucan and xylan increased up to 70º (Fig 9a) with the addition of the plasticiser. The plasticiser had varying effects on the tensile strength, tensile strain and Young's Modulus of the films. The tensile strength reached 9 MPa with 10% plasticiser but was negatively affected (< 4 mPa)with plasticiser addition of between 20-30% (Fig. 9b).The effect on the tensile strain was the same (~20 MPa) for MHH with plasticiser of 10-20% for the MHH (Fig 9c). The plasticiser effects on the tensile strain were noticeable with30- 40% addition of the plasticisers in pure XGN/XLN films (Fig 9c) with the largest effect realised with 40% plasticiser. There was a noticeable increase in the Young's Modulus from <500 MPa to > 700 MPa for the 10-20% plasticiser addition in the MHH films (9d). In contra'st, the films with XGN/XLN experienced a decrease in tensile strength from 9 MPa to < 6 MPa (9b). However, there was no noticeable effect on the Young's Modulus with up

to 20% plasticiser (~800 MPa) but a decrease (from 800 to 400-500 MPa) was observed with 30-40% plasticiser addition (Fig 9d).

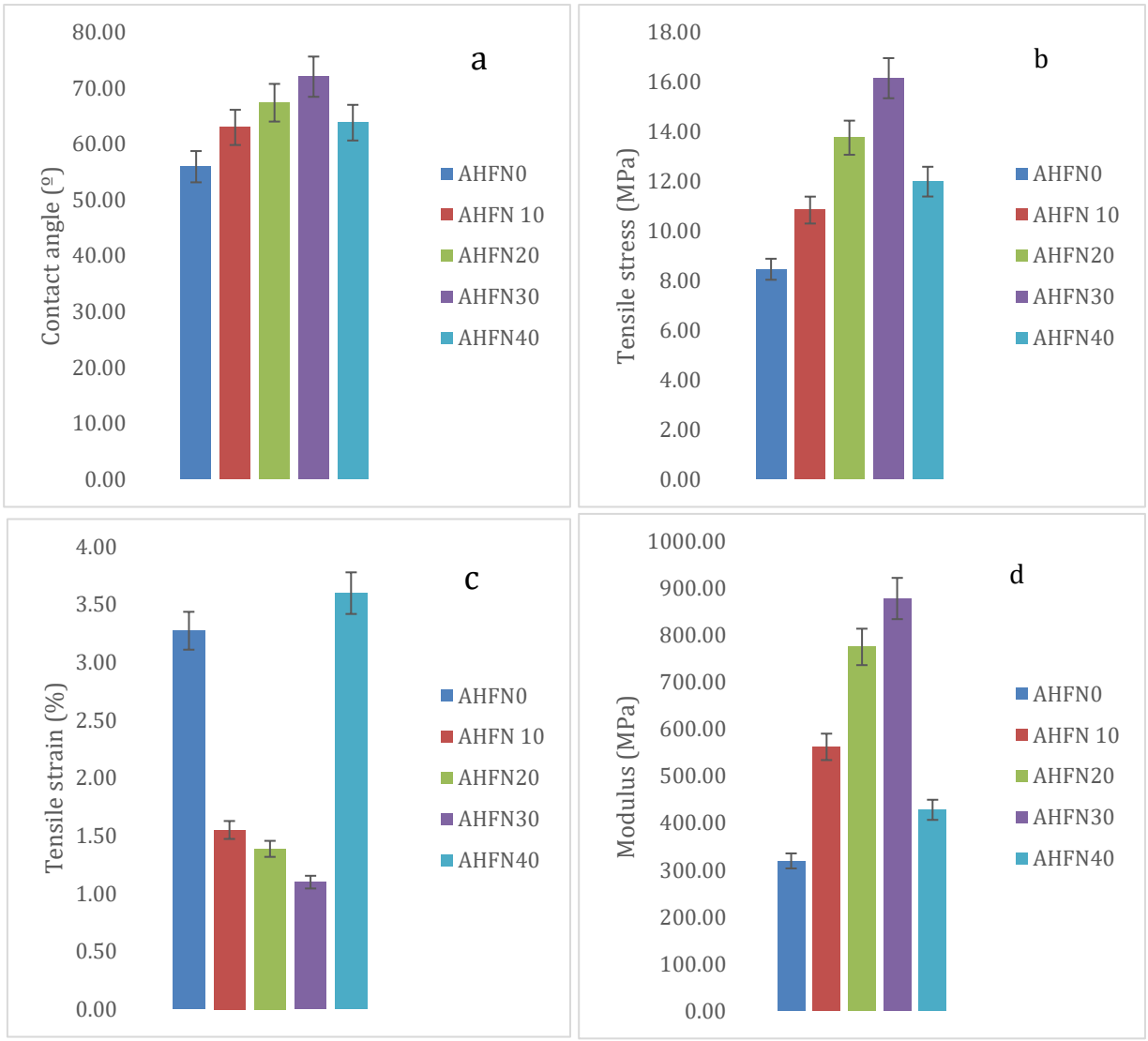

Figure 10: Effect of formic acid nanocellulose content on (a) Contact angle, (b) Tensile stress, (c) Tensile strain and (d) Modulus of acetylated mango seed husk hemicellulose: AHFN=Acetylated hemicellulose with 0, 10, 20, 30 and 40% formic acid nanocellulose. N/B Tensile strength of Low-density polyethylene films (7 – 25 MPa) (Bastarrachea, Dhawan and Sablani, 2011).

Hemicelluloses obtained from the alkaline method were acetylated before being combined with nanocellulose (FCNC) produced from the formic acid process to produce self-supporting and relatively hydrophobic biocomposites with water contact angles >70º upon addition of up to 30% FCNC (Fig. 10a). The tensile strength was > 16 mPa with 30% FCNC. The tensile strain decrease with 10-30% FCNC addition (Fig 10c) while the Young's Modulus increased ~900 MPa (Fig. 10d).

3.3.6 Valorization of mango seed kernel

The mango seed kernel composition consisted of ~4% lignin and 3% cellulose and hemicellulose and starch contents of ~18 and ~34% respectively. The low lignin content makes the kernel an attractive feedstock for the extraction of polyphenols. The optimized organosolv conditions 44% v/v ethanol and 54 °C gave a polyphenol extract yield of ~21% with total polyphenol and scavenging activity of 4298 mg Gallic acid equivalent (GAE)/100 g, and 83%, respectively. The hemicellulose and starch contents of the solid residue were ~20% and ~44%, respectively which were validated as shown in Table 17.

.

Table 17 Predicted and observed values for organosolv treatment of mango seed kernel at optimal conditions[a]

Variable	Predicted	Observed
Polyphenol yield (%)	21.75 ± 0.02	20.83 ± 1.23
Total polyphenol content mg (GAE)/100g	4267.81 ± 1.00	4342.70 ± 0.53
Scavenging activity (%)	82.77 ± 0.21	82.69 ±0.08
Starch content of residue (%)	44.14 ± 0.04	43.67 ± 0.76
Hemicellulose content of residue (%)	23.29 ± 0.02	20.11 ± 1.98

[a]Optimal conditions ~44% ethanol, and ~54 °C. GAE = Gallic acid equivalent

Hemicellulose with antioxidative activity (Fig. 11a) were obtained using an alkaline hydrolysis of destarched and organosolv treated mango seed kernel. The organosolv treatment was optimized to pre-extract polyphenols with minimal hemicelluloses degradation and formation of insoluble complexes with other cell components.

The mango seed kernel optimal alkaline conditions for extraction of hemicelluloses were 1.5 M NaOH concentration, 44 ºC temperature, and 3 h of reaction time. Under these conditions, the hemicellulose yield was 54% (starch-free basis) with lignin, total phenolic content, and uronic acid content of 5.05%, 2098 mg GAE/100g, and 12.53% (Fig 11a). Moreover, the hemicelluloses contained scavenging activity (54% of DPPH). Sugar composition analysis and FTIR confirmed the extract to be xyloglucan with a molecular weight of 108,163 g/mol compared with 2,372,886 g/mol for commercial tamarind seed xyloglucan (See Appendix). The maximum thermal degradation temperature was at 308 ºC, which was similar to the commercial xyloglucan (Fig 4a).

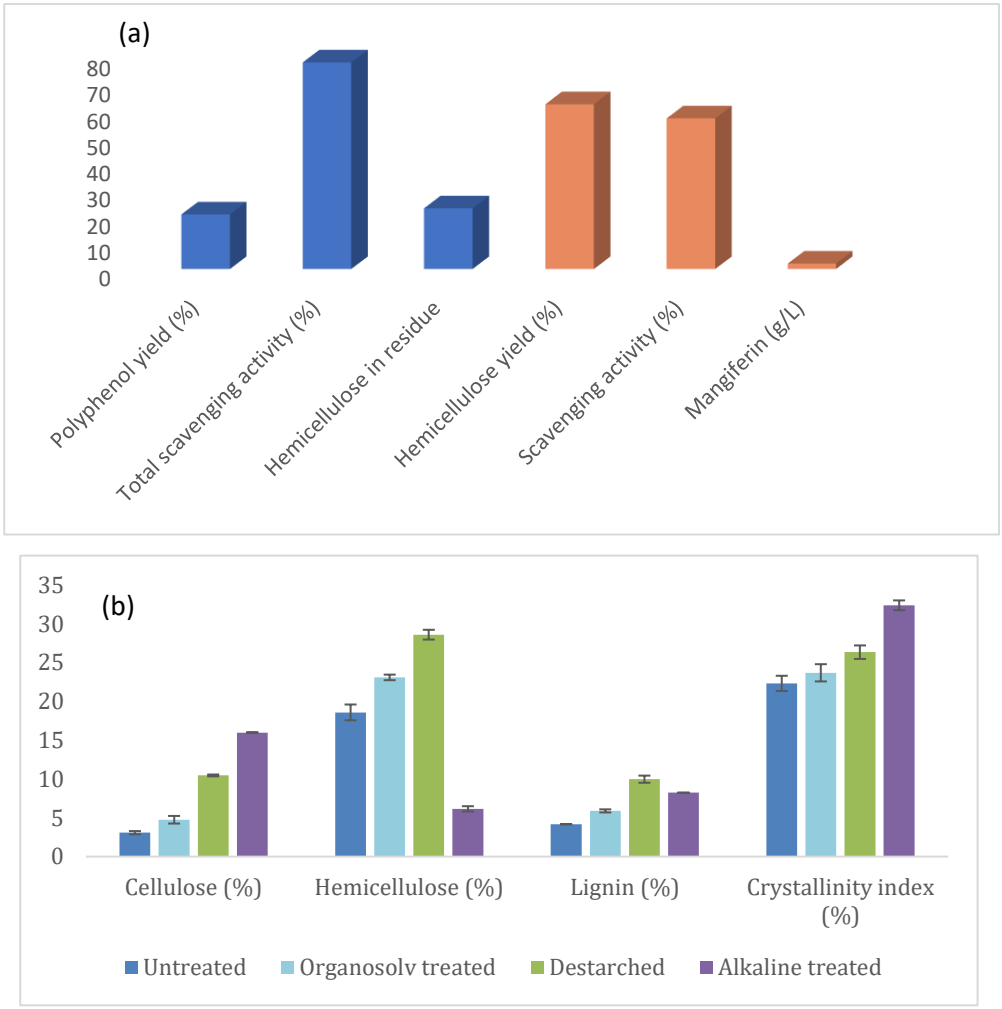

Figure 11 (a) Yield of polyphenol and hemicellulose and (b) properties of the residue after organosolv, destarching and alkaline treatment of mango kernel

The alkaline treatment left the mango seed kernel residue with the highest cellulose content of 15% and lowest hemicellulose content ~30% while increasing the crystallinity (Fig 11 b). The optimal conditions for hemicellulose extraction of 1.92 M, 44 °C, and 3 h (Table 18) were validated. The validation results were within the predicted with percentage error within 10% (Table 18), thus, confirming the repeatability of the results. The hemicelluloses recovered were stable based on the Zeta potential > -5 mV.

Table 18. Predicted and experimental yields and properties of bioproducts from mango seed kernel at optimum process conditions

	X_1, (M)	X_2, (°C)	X_3, (h)	Hemicellulose yield, (%)	Lignin content (%)	Total phenolic content (mg GAE/100g)	Antioxidant activity, (%)	Uronic acid content (%)
Optimum condition	1.92	44.00	3.0	~60	~5	~2100	~56	~8
validated conditions	1.92	44.00	3.0	~55	~5	~2100	~54	~7

X_1: NaOH concentration (M); X_2: Temperature (◦C); X_3: Extraction time (h)

4 Discussion

The compositions of the organic wastes from wheat (Table 8) and the mango residues (Tables 13 & 14) rendered these bioresources suitable feedstock for extraction of multiple high-value bioproducts. A total of seven potential high-value bioproducts were identified from the wheat (Tables 9, 10 & 11) and mango residues (Tables 13-18). There is potential to extract cellulose, hemicellulose, lignin, pectin, polyphenols, proteins and starch from the wheat residues and mango processing waste in high yields but only five of the seven bioproducts (lignin, polyphenols, hemicelluloses, cellulose and nanocellulose were optimized and validated. The remaining two products, starch and proteins were considered as byproducts.

Two fractionation routes, one for each of the residues (Figs. 2 & 3 for wheat and mango residues, respectively) showed that fractionating of the residues in a stepwise fashion increased the number of recovered functional bioproducts relative to what can be recovered in a single step. More importantly, the optimized stepwise approach combined with strategic selection of treatment combinations resulted in a triple gain. Thus, in addition to increasing the number of bioproducts, there was a reduction of impurities in the final product in this case the nanocellulose, and the bioproducts were obtained at reduced severe conditions. Thus, the key feature for the developed fractionation routes is the optimization of the fractionation conditions at each step to ensure maximum yield at conditions where functional properties of the targeted product as well as of the residues recovered are preserved for the efficient extraction of the subsequent product. Furthermore, the findings have shown that pretreatment processes, in this case, the two-stage alkaline and the homogenizer-assisted delignification, should be optimized to maximize the yield and functional properties of the nanocellulose. Notably, in most of the steps of the fractionation routes, the temperature and chemical / enzyme concentrations were the most influencing factors for obtaining the best product profile with acceptable yields and purity.

4.1 Wheat residues fractionation route

Wheat straw cellulose content (Table 8) suited nanocellulose production. The two-stage alkaline process, in particular, improved the composition and structure of the recovered wheat straw solid residues for nanocellulose production. However, the effectiveness of the treatment differed between the two types of wheat residues.

4.1.1 Effectiveness of two-stage alkaline pretreatment for production of nanocellulose from wheat residues

The two-stage alkaline treatment prepared the wheat straw for the production of relatively pure nanocellulose (Table 9). However, the treatment was less effective in removing hemicellulose and lignin from the wheat bran, even after the bran was de-starched (Table 8), thus, a hemicellulose-enriched nanocellulose was obtained from the bran which could suit special applications that can take advantage of the hemicellulose and lignin functionality, for example, applications in active packaging (Mugwagwa & Chimphango, 2020). Furthermore, the residual lignin could act as a plasticizer in the biocomposites (Fig. 8). Thus, it might not be necessary to completely remove the hemicellulose and lignin contents before producing nanocellulose if diversified functionalities are required in the biocomposite.

A positive effect of the two-stage alkaline treatment on the nanocellulose production was reflected by the high crystallinity of the cellulose-rich residue. The cellulose residue recovery from the treated wheat straw was 97% with a cellulose content that increased from 36 to 76% and crystallinity from 44 to 55% (Table 10). The generated a residue, in the case of the wheat straw that met the specifications found in the literature (Teixeira *et al*., 2010; Kallel *et al*., 2016; Espinosa *et al*., 2017). The minimum requirements for cellulose-rich pulp suitable for nanocellulose production are: cellulose content ≥ 62%, crystallinity index ≥ 48%, hemicelluloses content ≤ 23% and lignin ≤10% (Teixeira *et al*., 2010; Kallel *et al*., 2016; Espinosa *et al*., 2017). The release of the hemicelluloses, lignin and other components improved the purity and crystallinity of the nanocelluloses (Table 10). However, the greatest advantage is the ability to obtain, prior to nanocellulose, three bioproducts, thus, hemicelluloses, lignin, *p*-Coumaric acid (wheat straw) and *ferulic* acid (wheat bran), in higher yields than reported in the literature (Table 9). Moreover, the presence of hemicellulose could impede enzymatic hydrolysis (Penttilä *et al*., 2013a) The results show that total yields of the hemicelluloses and lignin from wheat straw were 77% and 68%, respectively (Table 9), and of the *p*-coumaric yield of 85% with an antioxidant activity of 45% (Table 10).

In the case of the wheat bran, over 70% of the lignin and 37% hemicelluloses were recovered accompanied by 66% *ferulic* acid with a 15% antioxidant activity at the mild-alkaline stage. In total, 52% hemicelluloses and 92% lignin were extracted from the wheat bran, which is not possible in conventional extraction processes. The results indicated that the two-stage alkaline treatment was

beneficial for the extraction of lignin and *ferulic* acid from the wheat bran. Furthermore, a cellulose recovery of 83% and an increase in crystallinity from 34% to 41% (Table 10) was achieved, which were not within the recommended levels for traditional nanocellulose production as per literature (Teixeira *et al*., 2010; Kallel *et al*., 2016; Espinosa *et al*., 2017). The presence of about 31% hemicelluloses in the residue, exceeded the maximum of 20% for nanocelluloses production (Penttilä *et al*., 2013b).

The residual hemicelluloses in the wheat bran solid residue reduced both the onset and the maximum thermal degradation temperatures (from 252 °C to 242 °C and 350 °C to 336 °C, respectively (Fig 4a). The thermal decomposition temperatures of the hemicelluloses (Fig. 4a) fell between 200 and 400 ºC. Notably, the release of the hemicelluloses, lignin and other components from the wheat bran still creates additional high-value chains (Table 10). The compositional analysis and thermal properties of the hemicelluloses, in particular, have high-value applications such as hydrogels and additives in papermaking (Farhat *et al*., 2017; Matavire, 2018).

4.1.2 Comparative analysis of nanocellulose production methods from wheat residues

The HCl and enzymatic methods as alternative to the conventional sulphuric acid, nanocellulose production methods resulted in similar yields, zeta potential and maximum thermal degradation temperatures that were higher than the traditional sulphuric acid treatment. In addition, the nanoparticles from the enzymatic treatment (ECN) were obtained at a relatively shorter treatment time (4.64 h) and lower temperature than the hydrochloric acid (HCN) produced nanoparticles (7.41 h) for the same yield. The short residence time (4.64 h) for the enzymatic treatment vs 7.41 h for the hydrochloric acid (Table 11) can be attributed to the combination of the mono-component enzyme (FiberCare R) and multicomponent enzyme (Viscozyme L) thus, making the enzymatic treatment a more attractive nanocellulose production method because of the reduced time and temperature (50 ^{o}C) required for processing.

4.2 Mango residues fractionation route

4.2.1 Mango residues as feedstock for multiproduct recovery in an integrated biorefinery

The mango wastes (peels, seed and husks) compositions (Tables 12 and 13) formed the basis for determining the suitable fractionation conditions for the individual fractions in an integrated biorefinery co-producing nanocellulose and other valuable products, in this case polyphenols, hemicelluloses, and lignin. The mango peels and kernel cellulose contents (Table 12) were not sufficient for nanocellulose production but were explored for anthocyanins, polyphenols and pectin in another project (Mugwagwa & Chimphango, 2019; Mugwagwa & Chimphango, 2020). Thus, the mango seed kernels composition, was deemed suitable for co-production of hemicelluloses and polyphenols, with starch as potential additional product. However, in this project starch was extracted

as a byproduct that was not recovered. The mango seed husks, (Table 13), were considered a suitable resource for hemicellulose, lignin and nanocellulose production because of being rich in cellulose content.

4.2.2 Step-wise multiproduct recovery from mango residues

Implementation of the multi-product fractionation route presented in Figure 3 yielded hemicelluloses and lignin in alkaline and homogenization - assisted organosolv processes, respectively. The initial alkaline conditions were optimized for the extraction of hemicellulose that would be suitable for thermal stable and self-supporting biocomposite (Fig 8). The hemicelluloses were identified to be a mixture of xylan and xyloglucan containing uronic acids and some lignin (Table 14). The customized dissolution of the XGN and XLN under the varying alkaline extraction conditions differentiated the functional properties of the hemicellulose in MSHs biocomposites (Fig. 8). Pure lignin (~ 70%) solubilized with >90% purity at ~148 ºC and 60% ethanol with 15 min homogenization (Bello & Chimphango, 2021), was obtained from the homogenization - assisted organosolv process.

The high shear homogenization assisted - organosolv (HSHO) process efficiently pre-treated/fractionated the alkaline treated mango seed husk into high purity lignin and cellulose-rich fibres in a biorefinery at lower temperatures when compared to the conventional organosolv process (Bello & Chimphango, 2021). The results from the desirability analysis (Statistica 13.2 software) showed that 60% ethanol, and temperature ~150 ºC with 15 min homogenization, gave maximum cellulose content and minimum lignin contents in the solid residue (Table 15). Validation experiments confirmed the findings (Table 15). The solubilized lignin yield and purity were comparable to those performed at an elevated temperature of 200 ºC when non-assisted (68.58% and 94.74%, respectively).

At the optimal HSHO process conditions, lignin fragments of purity >90%, with a molecular weight of 3247 g/mol and a maximum degradation temperature of 298 ºC was achieved (Bello & Chimphango, 2021). The solid pulp showed individual separated fibres with > 75% cellulose, <10% residual lignin, and <11% hemicelluloses which enhanced the formation of cellulose nanofibers (Fig 6). The high purity and molecular weight with the high thermal stability of the HSHO lignin make it suitable for a wide range of industrial applications including resins and carbon fibres (Bello & Chimphango, 2021).

4.2.3 Comparative analysis of nanocellulose production methods for mango husks

A mild and efficient organic acid method based on non-catalyzed formic acid treatment was successfully used to produce cellulose nanocrystals from unbleached mango husks (UMH) (Fig 6). The differences between the morphologies of the SCNC and FCNC (Fig 6) reflect the different reaction mechanisms between the inorganic and organic acids towards cellulose hydrolysis that can be used to diversify the functional properties. At the optimum conditions for the formic acid treatment

(30 mL/g and 8 h), high yields of crystalline and formylated spherical CNCs (Table 17) with better dispersion in different solvents (Fig 7) were obtained. The stability and dispersion of the CNC were tested for FCNC in DMAC, DMSO, and DMF. Figure 7 shows that the FCNC dispersed well in water, dimethylformamide (DMF), dimethylacetamide (DMAC), and dimethyl sulphoxide (DMSO) and was stable after 15 min of sonication except when in water, aggregation was evident after 24 at room temperature (Fig. 7).

Compared to the SCNC, the SFCN presented better thermal stability (T_{max}=361ºC) and hydrophobicity due to the surface formate groups (Table 16), making it suitable for thermal stable nanocomposites for application in industries such as biomedicine, food and cosmetics where thermal stability is required. Thus, the non-catalyzed formic acid hydrolysis method provides a greener approach for large-scale production of thermally stable, hydrophobic CNCs compared to the classical sulphuric acid method that is associated with environmental and technical problems due to the highly corrosive and toxic nature.

4.2.4 Functional and film - forming properties of bioproducts from mango husks

The alkaline extraction of hemicellulose from the mango seed husk has the potential for producing self-supporting films for diverse applications including food packaging. The hydrophobicity of the MHs films did not change with the addition of a plasticizer while that of the pure XGN/XLN composite showed a positive effect upon the addition of the plasticizer, attaining water contact angles of up to 70º (Fig 9a). The presence of lignin in the mango seed husk hemicellulose could have acted as a plasticizer to aid in film formation. This may explain the effects of the plasticizer on the tensile strength, tensile strength and Young's Modulus presented in Figures 9b-d. The plasticiser (10%) increased the tensile strength while 10-20% increase the Young's Modulus (Figs 9b & d). The mechanical properties of the biocomposite were improved by the addition of a plasticizer (Figs. 9a-d), which suggest that it is beneficial to have lignin as an inherent plasticizer. Nevertheless, with the addition of > 40% nanocellulose, both the tensile strength and modulus reduced. Therefore, the maximum nanocellulose addition should be limited to < 40%.

The hemicelluloses obtained from the alkaline process (MHHs) were acetylated before being combined with nanocellulose (FCNC) produced from the formic acid process to produce self-supporting and relatively hydrophobic biocomposites. The water contact angles >80º (Fig. 10a).The addition of the formic acid produced nanocellulose to acetylated mango seed husk hemicellulose (without plasticizer) improved the mechanical properties (Young's Modulus and tensile strength) and hydrophobicity of the films (high contact angles) compared to hemicellulose only (Figs. 10 b-d). The mechanical properties of the biocomposite compared well with those of the commercial low - density polyethylene (LDPE) that are used in food application (Bastarrachea, Dhawan & Sablani, 2011). The tensile strength and Young's Modulus were approximately 11MPa and 240 MPa, respectively. Overall, the mango seed husk offers important mixtures of biodegradable polymers (hemicellulose, lignin, nanocellulose) for film formulation for packaging application.

A self-supporting film with a maximum degradation temperature of 290 °C was obtained from the extracted hemicellulose envisaged for application in food packaging. In addition, biocomposite films produced using MHH with varying XGN and XLN presented higher thermal degradation temperatures than the commercial counterpart CXLN. Moreover, it was observed that XGN in any ratio during the production of xylan composites films could improve the overall thermal stability of the film (Fig. 8). Thus, feedstocks such as MSHs with varying types of hemicelluloses, present ideal feedstocks for obtaining hemicellulose extracts with diversified functionalities. However, the co-existence of different types of hemicelluloses with lignin and cellulose warrants investigation for possible integration in a biorefinery setup. Also, the role of residual lignin in biocomposites requires further investigation. This study has demonstrated a novel approach for diversifying hemicellulose applications and adding value to mango waste.

4.2.5 Potential industrial applications of the nanocellulose and the co-products from wheat straw and wheat bran

The fractionation routes developed for the wheat straw and wheat bran were optimized to produce five bio products, which in literature have shown to have ready markets. Table 19 provides a list of some of the applications. The hemicelluloses obtained can be applied in the papermaking industry as an additive to improve its mechanical properties. The nanocelluloses produced (SCN, HCN, and ECN) presents the potential to be applied in aerogels, hydrogels and wastewater treatment.

Table 19: Potential applications of bioproducts from wheat straw and wheat bran

Product	Potential applications	References
Hemicelluloses	Hydrogels and additive in paper making industries	Yuan *et al*. (2016); Farhat *et al*., (2017); Matavire, (2018)
Lignin	Polymer composite materials and partial replacement in phenolic resins	Li & Mcdonald (2014); Watkins *et al*., (2015)
Ferulic acid	As precursor in vanillin production, pharmaceutical industry	Tapin *et al*. (2006) ; Ou *et al*., (2007)
p-Coumaric acid	As a precursor in *p*-hydroxybenzoic acid the production, enhancing foaming abilities and applications in emulsions	Jiang *et al*. (2016b); Phongthai *et al*., (2016)
Nanocellulose	Aerogels, hydrogels, and waste-water treatment	(France *et al*. (2017); Shak *et al*. (2018)

The thermal decomposition temperatures of the hemicelluloses (Fig. 4a) and lignin (Fig. 4b) between 200-400ºC is a reflection of the functional properties of the two products. The compositional analysis and thermal properties of the hemicelluloses, in particular, shows potential for application in

thermal stable hydrogels formation and other industrial applications such ascoatings in papermaking industries (Farhat *et al*., 2017; Matavire, 2018). Furthermore, the thermal stability and anti-oxidant activity of the extracted hemicelluloses, would suit applications such as the formulation of active food packaging.

The extraction of polyphenols of high antioxidant activity from mango seed kernel for application in both the food and non-food industries, while obtaining a solid residue of high starch and hemicellulose content for further extraction and valorization. The kernel residue can be used for the production of multifunctional composites or bioproducts. Therefore, higher economic exploits for the mango seed kernel can be realized through the biorefinery concept. The efficient extraction of hemicellulose with antioxidant activity provides a promising feedstock for the formulation of active packaging without the addition of external antioxidants for application in many industries including the food, paper making, and biomedical fields just to name a few.

5 Conclusion

There is more value that can be obtained from wheat and mango - based organic waste in step-wise integrated biorefineries in which each step is optimized for the extracted bioproduct and the residue than in conventional biorefineries. A two-stage alkaline treatment has demonstrated to be a potential novel pretreatment method for preparing the wheat residues for nanocellulose production under reduced severity of the process conditions while increasing the number, yield and purity of the bioproducts recovered. The step-wise fractionation routes, with optimization of each step have demonstrated that five bioproducts (lignin, polyphenols, hemicelluloses and nanocelluloses) could be produced in high yields and purity. The findings have provided a basis for selecting a combination of bioproducts with the potential to give maximum economic value from the organic wastes with environmental gains. However, the techno-economic feasibility and the environmental sustainability of implementing such biorefineries either at the place where the residues are generated or as stand-alone entities need further investigation. Furthermore, more applications of the bioproducts and byproducts and the economic contribution to the biorefinery need to be investigated. For instance, the monomers including glucose from the enzymatic treatment (14.28 g/l) could be used for ethanol production generating a theoretical yield of 7.3 g/l.

6 Acknowledgments

The Authors would like to acknowledge the contributions of the following:

- DST/ CSIR Waste Road Map- For financial support
- National Research Foundation (NRF)- For additional financial support on the project
- Central Analytical Facility (SU)- For the analytical service in sample analysis
- Process engineering Department Analytical Laboratory (SU)- For sample analysis
- Process Engineering Department Technical Staff (SU)- for assisting with sample preparations and running of equipment
- Wood Science Department (SU)- For organic waste sample preparation and provision of access to digesters and other preparatory equipment
- Polymer Science Department (SU)- For sample and bioproducts analysis
- Mango Processors Hoedspruit fruit processors (South Africa) for providing the initial mango seeds samples
- Eureka Mills- Supply of wheat bran
- Ms Fatimatu Bello and Mr Regan Ceaser (Postgraduate students in the Process Engineering Department at Stellenbosch University) who conducted the experiments and wrote reports and papers that have been the basis of this report.
- Prof Maya John (CSIR) for the initial collaboration on the project
- Prof Johann Görgens (SU) for co-supervision and grant-linked funding of the students
- Ms Juliana Steyl & Ms Anita Kleinschmidt for the administration support
- Post-doctoral students: Dr. M Namane; Dr. J Louw & Dr. LR Mugwagwa for initial work and support to the students.
- Process engineering Bioresource Research Group – For student intellectual support and sharing of equipment and resources.

7 REFERENCES

Agbor, V.B., Cicek, N., Sparling, R., Berlin, A. and Levin, D.B. (2011) Biomass pretreatment: Fundamentals toward application, *Biotechnology Advances*., 29(6), pp. 675–685. doi: 10.1016/j.biotechadv.2011.05.005

Ajila, C. M., Bhat, S. G. and Prasada Rao, U. J. S. (2007a) Valuable components of raw and ripe peels from two Indian mango varieties, *Food Chemistry*, 102(4), pp. 1006–1011. doi: 10.1016/j.foodchem.2006.06.036.

Ajila, C.M., Naidu, K.A., Bhat, S.G. and Rao, U.P. (2007b). Bioactive compounds and antioxidant potential of mango peel extract. *Food chemistry*, *105*(3), pp.982-988. doi: 10.1016/j.foodchem.2007.04.052.

Alemdar, A. and Sain, M. (2008) Isolation and characterization of nanofibers from agricultural residues - Wheat straw and soy hulls, *Bioresource Technology*, 99(6), pp. 1664–1671. doi: 10.1016/j.biortech.2007.04.029.

Arora, A., Banerjee, J., Vijayaraghavan, R., MacFarlane, D. and Patti, A.F. (2018). Process design and techno-economic analysis of an integrated mango processing waste biorefinery. *Industrial Crops and Products*, *116*, pp.24-34,. doi: 10.1016/j.indcrop.2018.02.061.

Ayrilmis, N., Ashori, A. and Kwon, J. H. (2016). Properties and Utilization of Plant Fibers and Nanocellulose for Thermoplastic Composites, *Polyethylene-Based Biocomposites and Bionanocomposites*, pp. 405–428. doi: 10.1002/9781119038467.ch11.

Banerjee, J., Vijayaraghavan, R., Arora, A., MacFarlane, D.R. and Patti, A.F. (2016). Lemon juice based extraction of pectin from mango peels: Waste to wealth by sustainable approaches. *ACS Sustain. Chem. Eng.*, 4(11), pp. 5915–5920

Barman, D.N., Haque, M.A., Kang, T.H., Kim, M.K., Kim, J., Kim, H. and Yun, H.D. (2012). Alkali pretreatment of wheat straw (*Triticum aestivum*) at boiling temperature for producing a bioethanol precursor. *Bioscience Biotechnology and Biochemistry*, 76(12), pp. 2201–2207. doi: 10.1271/bbb.120480.

Bastarrachea, L., Dhawan, S. and Sablani, S. S. (2011) Engineering Properties of Polymeric-Based Antimicrobial Films for Food Packaging, *Food Engineering Reviews*, pp. 79–93. doi: 10.1007/s12393-011-9034-8.

Bataillon, M., Mathaly, P., Cardinali, A.N. and Duchiron, F. (1998). Extraction and purification of arabinoxylan from destarched wheat bran in a pilot scale., *Industrial Crops and Products*, 8, pp. 37–43. https://doi.org/10.1016/S0926-6690(97)10002-4

Bello, F. and Chimphango, A. (2021). Optimization of lignin extraction from alkaline treated mango seed husk by high shear homogenization-assisted organosolv process using response surface methodology. *International Journal of Biological Macromolecules*, *167*, pp.1379-1392. https://doi.org/10.1016/j.ijbiomac.2020.11.092

Boz, H. (2015) Ferulic acid in cereals - A review, *Czech Journal of Food Sciences*, 33(1), pp. 1–7. doi: 10.17221/401/2014-CJFS.

Brienzo, M., Siqueira, A.F. and Milagres, A.M.F. (2009). Search for optimum conditions of sugarcane bagasse hemicellulose extraction. *Biochemical Engineering Journal*, *46*(2), pp.199-204. https://doi.org/10.1016/j.bej.2009.05.012

Buranov, A. U. and Mazza, G. (2009) Extraction and purification of ferulic acid from flax shives , wheat and corn bran by alkaline hydrolysis and pressurised solvents, *Food Chemistry*. Elsevier Ltd, 115(4), pp. 1542–1548. doi: 10.1016/j.foodchem.2009.01.059.

Ceaser, R. and Chimphango, A.F. (2021). Comparative analysis of physical and functional properties of cellulose nanofibers isolated from alkaline pre-treated wheat straw in optimized hydrochloric acid and enzymatic processes. *International Journal of Biological Macromolecules*, *171*, pp.331-342. https://doi.org/10.1016/j.ijbiomac.2021.01.018

Cebreiros, F., Guigou, M. D. and Cabrera, M. N. (2017). Integrated forest biorefineries: Recovery of acetic acid as a by-product from eucalyptus wood hemicellulosic hydrolysates by solvent extraction, *Industrial Crops & Products*. Elsevier, 109, pp. 101–108. doi: 10.1016/j.indcrop.2017.08.012.

Cheng, M., Qin, Z., Chen, Y., Hu, S., Ren, Z. and Zhu, M. (2017). Efficient extraction of cellulose nanocrystals through hydrochloric acid hydrolysis catalyzed by inorganic chlorides under hydrothermal conditions. *ACS Sustainable Chememical Engineering*, 5, pp. 4656–4664. DOI 10.1021/acssuschemeng.6b03194.

Chimphango, A.F., van Zyl, W.H. and Görgens, J.F., (2012). Isolation, characterization and enzymatic modification of water soluble xylans from *Eucalyptus grandis* wood and sugarcane bagasse. *Journal of Chemical Technology & Biotechnology*, *87*(10), pp.1419-1429. https://doi.org/10.1002/jctb.3761

Chinga-Carrasco, G. (2011) Cellulose fibres, nanofibrils and microfibrils: The morphological sequence of MFC components from a plant physiology and fibre technology point of view., *Nanoscale research letters*, 6(1), p. 417. doi: 10.1186/1556-276X-6-417

Cordeiro, E.M., Nunes, Y.L., Mattos, A.L., Rosa, M.F., de sá M. Sousa Filho, M. and Ito, E.N. (2014). Polymer biocomposites and nanobiocomposites obtained from mango seeds. In *Macromolecular Symposia*. 344 (1), pp. 39–54. doi: 10.1002/masy.201300217

Cripwell, R., Favaro, L., Rose, S.H., Basaglia, M., Cagnin, L., Casella, S. and van Zyl, W. (2015). Utilisation of wheat bran as a substrate for bioethanol production using recombinant cellulases and amylolytic yeast. *Applied Energy*, 160, pp. 610–617. DOI 10.1016/j.apenergy.2015.09.062.

Daiber, K. H. (1975) Enzyme inhibition by polyphenols of sorghum grain and malt, *Journal of the Science of Food and Agriculture*, 26(9), pp. 1399–1411. doi: 10.1002/jsfa.2740260920.

da Silva Meireles, C., Rodrigues Filho, G., Ferreira Jr, M.F., Cerqueira, D.A., Assunção, R.M.N., Ribeiro, E.A.M., Poletto, P. and Zeni, M. (2010). Characterization of asymmetric membranes of cellulose acetate from biomass: Newspaper and mango seed. *Carbohydrate polymers*, *80*(3), pp.954-961. pp. 954–961. doi: 10.1016/j.carbpol.2010.01.012.

de Morais Teixeira, E., Corrêa, A.C., Manzoli, A., de Lima Leite, F., de Oliveira, C.R. and Mattoso, L.H.C. (2010). Cellulose nanofibers from white and naturally colored cotton fibers. *Cellulose*, *17*(3), pp.595-606. doi: 10.1007/s10570-010-9403-0

Department of Agriculture Forestry and Fisheries (2011) *A profile of the South African table grape market value chain*. doi: 10.1007/s13398-014-0173-7.2.

Dorta, E., Lobo, M Gloria and Gonzalez, M. (2012) Reutilization of mango byproducts: Study of the effect of extraction solvent and temperature on their antioxidant properties, *Journal of Food Science*, 71(1), pp. 80–89. doi: 10.1111/j.1750-3841.2011.02477.x

Du, H., Liu, C., Zhang, Y., Yu, G., Si, C. and Li, B. (2016). Preparation and characterization of functional cellulose nanofibrils via formic acid hydrolysis pretreatment and the followed high-pressure homogenization. *Ind. Crop. Prod*., 94, 736–745. DOI 10.1016/j.indcrop.2016.09.059.

Dzigbor, A. and Chimphango, A. (2019) Production and optimization of NaCl-activated carbon from mango seed using response surface methodology, *Biomass Conversion and Biorefinery*. Biomass Conversion and Biorefinery, 9(2), pp. 421–431. doi: 10.1007/s13399-018-0361-3.

Egüés, I., Sanchez, C., Mondragon, I. and Labidi, J. (2012). Separation and purification of hemicellulose by ultrafiltration. *Industrial & engineering chemistry research*, *51*(1), pp.523-530. dx.doi.org/10.1021/ie202304q

Egüés, I., Sanchez, C., Mondragon, I. and Labidi, J. (2012). Effect of alkaline and autohydrolysis processes on the purity of obtained hemicelluloses from corn stalks. *Bioresource technology*, *103*(1), pp.239-248. https://doi.org/10.1016/j.biortech.2011.09.139

Eichhorn, S.J., Dufresne, A., Aranguren, M., Marcovich, N.E., Capadona, J.R., Rowan, S.J., Weder, C., Thielemans, W., Roman, M., Renneckar, S. and Gindl, W. (2010). Current international research into cellulose nanofibres and nanocomposites. *Journal of materials science*, *45*(1), pp.1-33. https://doi.org/10.1007/s10853-009-3874-0

Espinosa, E., Sánchez, R., Otero, R., Domínguez-robles, J. and Rodríguez, A. (2017). A comparative study of the suitability of different cereal straws for lignocellulose nanofibers isolation. *International Journal of Biological Macromolecules*, 103, 990–999. DOI 10.1016/j.ijbiomac.2017.05.156.

Farhat, W., Venditti, R., Quick, A., Taha, M., Mignard, N., Becquart, F. and Ayoub, A. (2017). Hemicellulose extraction and characterization for applications in paper coatings and adhesives. *Industrial Crops and Products*., 107, pp. 370–377. doi: 10.1016/j.indcrop.2017.05.055.

Favaro, L., Basaglia, M. and Casella, S. (2012) Processing wheat bran into ethanol using mild treatments and highly fermentative yeasts, *Biomass and Bioenergy*, 46, pp. 605–617. doi:

10.1016/j.biombioe.2012.07.001

France, K. J. De, Hoare, T. and Cranston, E. D. (2017) Review of Hydrogels and Aerogels Containing Nanocellulose, *Chemistry of Materials*, 29, pp. 4609–4631. doi: 10.1021/acs.chemmater.7b00531

Hames, B., Scarlata, C. and Sluiter, A. (2008). *Determination of Protein Content in Biomass:* (pp. 1-5). Golden, CO: National Renewable Energy Laboratory. Report No.TP-510-42625. Doi:10.1.1.693.7113

Henrique, M. A., Silvrio, H. A., Flauzino Neto, W. P. and Pasquini D. (2013). Valorization of an agro-industrial waste, mango seed, by the extraction and characterization of its cellulose nanocrystals, *Journal of Environmental Management*. 121, pp. 202–209. doi: 10.1016/j.jenvman.2013.02.054.

Hosseinian, F.S. and Mazza, G. (2009). Triticale bran and straw: Potential new sources of phenolic acids, proanthocyanidins, and lignans. *Journal of Functional Foods*. Elsevier Ltd, 1(1), pp. 57–64. doi: 10.1016/j.jff.2008.09.009.

Hou, F., Ding, W., Qu, W., Olayemi, A., Xiong, F., Zhang, W. (2017). Alkali solution extraction of rice residue protein isolates : Influence of alkali concentration on protein functional , structural properties and lysinoalanine formation. Food Chemistry. 218, pp. 207–215. https://doi.org/10.1016/j.foodchem.2016.09.064

Jaisamut, K., Paulová, L., Patáková, P., Rychtera, M. and Melzoch, K. (2013). Optimization of alkali pretreatment of wheat straw to be used as substrate for biofuels production. *Plant, Soil and Environment*, 59(12), pp. 537–542

Janker-obermeier, I., Sieber, V., Faulstich, M. and Schieder, D. (2012). Solubilization of hemicellulose and lignin from wheat straw through microwave-assisted alkali treatment. *Industrial Crops & Products*, 39, pp. 198–203, DOI 10.1016/j.indcrop.2012.02.022.

Jiang, H., Zeng, Y., Nie, H., Li, Y., Ding, J. and Zhou, H. (2016a). NaOH pretreatment of wheat straw at a mesophilic temperature: effect on hydrolysis and loss of organic carbon. *Polish Journal of Enviromental Studies*, 25, 1541–1548. DOI 10.15244/pjoes/62647

Jiang, K., Li, L., Long, L. and Ding, S. (2016b). Comparison of alkali treatments for efficient release of *p*-coumaric acid and enzymatic saccharification of sorghum pith. *Bioresource technology*, *207*, pp.1-10. https://doi.org/10.1016/j.biortech.2016.01.116

Joglekar, S.N., Pathak, P.D., Mandavgane, S.A. and Kulkarni, B.D., 2019. Process of fruit peel waste biorefinery: a case study of citrus waste biorefinery, its environmental impacts and recommendations. *Environmental Science and Pollution Research*, *26*(34), pp.34713-34722. https://doi.org/10.1007/s11356-019-04196-0

Johar, N., Ahmad, I. and Dufresne, A. (2012) Extraction, preparation and characterization of cellulose fibres and nanocrystals from rice husk, *Industrial Crops and Products*, 37(1), pp. 93–99. doi: 10.1016/j.indcrop.2011.12.016.

Kallel, F., Bettaieb, F., Khiari, R., García, A., Bras, J. and Chaabouni, S.E. (2016). Isolation and structural characterization of cellulose nanocrystals extracted from garlic straw residues. *Industrial Crops and Products, 87,* pp.287-296. doi: 10.1016/j.indcrop.2016.04.060.

Karp, E.M., Donohoe, B.S., OBrien, M.H., Ciesielski, P.N., Mittal, A., Biddy, M.J. and Beckham, G.T. (2014). Alkaline pretreatment of corn stover: Bench-scale fractionation and stream characterization. *ACS Sustainable Chemistry and Engineering*, 2, 1481–1491. DOI 10.1021/sc500126u.

Kaushik, A. and Singh, M. (2011) Isolation and characterization of cellulose nanofibrils from wheat straw using steam explosion coupled with high shear homogenization, *Carbohydrate Research*, 346(1), pp. 76–85. doi: 10.1016/j.carres.2010.10.020

Kaur, M., Singh, N., Sandhu, K. S. and Guraya, H. S. (2004). Physicochemical, morphological, thermal and rheological properties of starches separated from kernels of some Indian mango cultivars (Mangifera indica L.). *Food Chem.*, 85(1), 131–140

Khan, T.S. and Mubeen, U. (2012). Wheat Straw : A Pragmatic Overview. *Current Research Journal of Biological Sciences 4*(6), pp.673-675. ISSN: 2041-0778

Kittiphoom, S. (2012) Utilization of mango seed, *International Food Research Journal*, 19(4), pp. 1325–1335

Kock, J. L. F. *et al.* (1985) Extraction of polyphenols and hydrolysis of birdproof sorghum starch, *Journal of the Science of Food and Agriculture*, 36(11), pp. 1140–1144. doi: 10.1002/jsfa.2740361118.

Kumar, A., Negi, Y.S., Choudhary, V., Bhardwaj, N.K., 2014. Characterization of Cellulose Nanocrystals Produced by Acid-Hydrolysis from Sugarcane Bagasse as Agro-Waste. *Journal of materials physics and chemistry* 2 (1), pp. 1–8. https://doi.org/10.12691/jmpc-2-1-1

Lee, D., Owens, V.N., Boe, A. and Jeranyama, P. (2007). Composition of herbaceous biomass feedstocks. South Dakota State University Publication, SGINC1-07. *Brookings,* South Dakota

Lee, H. V, Hamid, S. B. A. and Zain, S. K. (2014a) Conversion of Lignocellulosic Biomass to Nanocellulose : Structure and Chemical Process, *Scientific World Journal*, pp. 1–14. doi: 10.1155/2014/631013.

Lee, K.Y., Aitomäki, Y., Berglund, L.A., Oksman, K. and Bismarck, A. (2014b). On the use of nanocellulose as reinforcement in polymer matrix composites. *Composites Science and Technology, 105*, pp.15-27. https://doi.org/10.1016/j.compscitech.2014.08.032

Li, H. and Mcdonald, A. G. (2014) Fractionation and characterization of industrial lignins, *Industrial Crops & Products*. Elsevier B.V., 62, pp. 67–76. doi: 10.1016/j.indcrop.2014.08.013.

Liu, Q. (2017). Isolation and characterization of nanocelluloses from wheat straw and their application in agricultural water-saving materials. University of Liège. http://hdl.handle.net/2268/216283

Liu, K.X., Li, H.Q., Zhang, J., Zhang, Z.G. and Xu, J. (2016). The effect of non-structural components and lignin on hemicellulose extraction. *Bioresour. Technol.*, 214, 755–760

Masibo, M. and Qian, H. (2008) Major mango polyphenols and their potential significance to human health, *Comprehensive Reviews in Food Science and Food Safety*, 7(4), pp. 309–319. doi: 10.1111/j.1541-4337.2008.00047.x.

Matavire, T.O. (2018). Extraction and modification of hemicellulose from wheat bran to produce entrapment materials for the controlled release of chemicals and bioactive substances. Stellenbosch University.

Max, B., María, A., Belén, A., Converti, A. and Manuel, J. (2009). Ferulic acid and p -coumaric acid solubilization by alkaline hydrolysis of the solid residue obtained after acid prehydrolysis of vine shoot prunings : Effect of the hydroxide and pH. *Biochem. Eng. J.*, 43, pp. 129–134. DOI 10.1016/j.bej.2008.09.015.

Menon, L., Dutta Majumdar, S. and Ravi, U. (2014) Mango (Mangifera indica L.) kernel flour as a potential ingredient in the development of composite flour bread, *Indian Journal of Natural Products and Resources*, 5(1), pp. 75–82. http://nopr.niscair.res.in/handle/123456789/27481

Merali, Z., Ho, J.D., Collins, S.R.A., Gall, G. Le, Elliston, A., Käsper, A. and Waldron, K.W. (2013). Characterization of cell wall components of wheat bran following hydrothermal pretreatment and fractionation. *Bioresource Technology*, 131, pp. 226–234. DOI 10.1016/j.biortech.2012.12.023.

Moran, J.I., Alvarez, V.A., Cyras, V.P. and Vazquez, A. (2008). Extraction of cellulose and preparation of nanocellulose from sisal fibers. *Cellulose*, 15, pp. 149–159. DOI 10.1007/s10570-007-9145-9.

Moniz, P., Lino, J., Duarte, L.C., Roseiro, L., Boeriu, C.G., Pereira, H. and Carvalheiro, F.. (2015) Fractionation of hemicelluloses and lignin from rice straw by combining autohydrolysis and optimised mild organosolv delignification, *BioResources*. North Carolina State University, 10(2), pp. 2626–2641. doi: 10.15376/biores.10.2.2626-2641

Mugwagwa, L.R. and Chimphango, A.F.A. (2019). Box-Behnken design based multi-objective optimization of sequential extraction of pectin and anthocyanins from mango peels. *Carbohydrate polymers*, *219*, pp.29-38. https://doi.org/10.1016/j.carbpol.2019.05.015

Mugwagwa, L.R. and Chimphango, A.F. (2020). Enhancing the functional properties of acetylated hemicellulose films for active food packaging using acetylated nanocellulose reinforcement and polycaprolactone coating. *Food Packaging and Shelf Life*, *24*, p.100481. https://doi.org/10.1016/j.fpsl.2020.100481

Nilsson, C. (2017). Preparation and characterization of nanocellulose from wheat bran. Lund University. Available at: https://lup.lub.lu.se/student-papers/search/publication/8906333

Ntshangase, T., Phaleng, L. and Potelwa, Y. (2017). South Africa fruit trade flow. NAMC, Issue No. 26, Pretoria, South Africa.

Nwadiogb, J.O., Igwe, A.A., Okoye, N.H. and Chime C.C. (2015). Extraction and characterization of microcrystalline cellulose from mango kernel: A waste management approach. *Der Pharma Chem.*,7(11), 1–7.

Onipe, O.O., Jideani, A.I.O. and Beswa, D. (2015). Composition and functionality of wheat bran and its application in some cereal food products. *International Journal of Food Science and Technology*, 50(12), pp. 2509–2518. doi: 10.1111/ijfs.12935

Ou, S., Luo, Y., Xue, F., Huang, C., Zhang, N. and Liu, Z. (2007). Seperation and purification of ferulic acid in alkaline-hydrolysate from sugarcane bagasse by activated charcoal adsorption / anion macroporous resin exchange chromatography. *Journal of Food Engineering*, 78, pp. 1298–1304. doi: 10.1016/j.jfoodeng.2005.12.037.

Ou, S.Y., Teng, J.W., Zhao, Y.Y. and Zhao, J. (2012). *p*-Coumaric acid production from lignocelluloses. *Phenolic Acids: Composition, Applications and Health Benefits*, pp. 63–71.

Pan, G.X., Bolton, J.L., Leary, G.J., Street, K.C. and Tn, C. (1998). Determination of ferulic and p - coumaric acids in wheat straw and the amounts released by mild acid and alkaline peroxide treatment. *J. Agric. Food Chem.*, 46, pp. 5283–5288. DOI 10.1021/jf980608f.

Peng, Y. and Wu, S. (2010). The structural and thermal characteristics of wheat straw hemicellulose. *J ournal of Analytical and Applied Pyrolysis*, 88(2), pp. 134–139. DOI 10.1016/j.jaap.2010.03.006.

Penttilä, P. A., Várnai, A., Pere, J., Tammelin, T., Salmén, L., Siika-Aho, M., Viikari, L. and Serimaa, R.*et al.* (2013a) Xylan as limiting factor in enzymatic hydrolysis of nanocellulose, *Bioresource Technology*, 129, pp. 135–141. doi: 10.1016/j.biortech.2012.11.017.

Penttilä, Paavo A., Várnai, A., Fernández, M., Kontro, I., Liljeström, V., Lindner, P., Siika-aho, M., Viikari, L. and Serimaa, R. (2013b). Small-angle scattering study of structural changes in the microfibril network of nanocellulose during enzymatic hydrolysis. *Cellulose*, 20, pp. 1031–1040. DOI 10.1007/s10570-013-9899-1

Phongthai, S., Lim, S.T. and Rawdkuen, S. (2016). Optimization of microwave-assisted extraction of rice bran protein and its hydrolysates properties. *Journal of Cereal Science*, 70, pp. 146–154. doi: 10.1016/j.jcs.2016.06.001.

Rabetafika, H.N., Bchir, B., Blecker, C., Paquot, M. and Wathelet, B. (2014). Comparative study of alkaline extraction process of hemicelluloses from pear pomace. *Biomass and Bioenergy*, 61, 254–264. DOI 10.1016/j.biombioe.2013.12.022.

Rosa, S.M.L., Rehman, N., De Miranda, M.I.G., Nachtigall, S.M.B. and Bica, C.I.D. (2012). Chlorine-free extraction of cellulose from rice husk and whisker isolation. *Carbohydrate Polymers*. Elsevier Ltd., 87(2), pp. 1131–1138. doi: 10.1016/j.carbpol.2011.08.084

Sánchez-Bastardo, N., Cocero, M.J. and Alonso, E. (2013). Heterogenous catalysis for the extraction of arabinoxylans from wheat bran. *Journal of Chemical Information and Modeling*, 53(9), pp. 1689–1699. doi: 10.1017/CBO9781107415324.004.

Shak, K.P.Y., Pang, Y.L. and Mah, S.K. (2018). Nanocellulose: Recent advances and its prospects in environmental remediation. *Beilstein journal of nanotechnology*, *9*(1), pp.2479-2498. https://doi.org/10.3762/bjnano.9.232

Shibuya, H. and Hayashi, T. (2008). Manufacture of cellulose nanofibers by enzymatic treatment and cellulose nanofibers manufactured thereby. *JP2006-337350*, *13*.

Sipponen, M.H., Pihlajaniemi, V., Sipponen, S., Pastinen, O. and Laakso, S. (2014). Autohydrolysis and aqueous ammonia extraction of wheat straw : Effect of treatment severity on yield and structure of hemicellulose and lignin. *RSC Advances*, 4, pp. 23177–23184. doi: 10.1039/c4ra03236e.

Shatkin, J.O.A., Wegner, T.H. and Bilek, E.M.T.E.D. (2014). Market projections of cellulose nanomaterial-enabled products- Part 1: Applications. 13(5), 9–16.

Sluiter, A., Hames, B., Ruiz, R., Scarlata, C., Sluiter, J., Templeton, D. and Crocker, D. (2012). Determination of structural carbohydrates and lignin in biomass determination of structural carbohydrates and lignin in biomass. *National Renewable Energy Laboratory*, 1–15.

Sun, R.C. (2010). *Cereal Straw as a Resource for Sustainable Biomaterials and Biofuels*, 1st ed. Oxford.

Sun, Y. and Cheng, J. (2002). Hydrolysis of lignocellulosic materials for ethanol production: a review. *Bioresource technology*, 83(1), pp. 1–11. doi: 10.1016/S0960-8524(01)00212-7.

Sun, R., Lawther, J.M. and Banks, W.B. (1995). Influence of alkaline pre-treatments on the cell wall components of wheat straw. *Industrial Crops and Products*, 4, pp. 127–145. https://doi.org/10.1016/0926-6690(95)00025-8

Sun, X.F., Sun, R., Fowler, P. and Baird, M.S. (2005). Extraction and characterization of original lignin and hemicelluloses from wheat straw. *Journal of Agricultural and Food Chemistry*, (53), pp. 860–870. doi: 10.1021/jf040456q.

Tahir, M.I., Khalique, A., Pasha, T.N. and Bhatti, J.A. (2002). Comparative evaluation of maize bran , wheat bran and rice bran on milk production of holstein friesian cattle. *International Journal of Agricultural and Biology*, 4(4), pp. 559–560.

Tapin, S. *et al.* (2006) Feruloyl Esterase Utilization for Simultaneous Processing of Nonwood Plants into Phenolic Compounds and Pulp Fibers, *Journal of Agricultural and Food Chemistry*, 54, pp. 3697–3703

Teixeira, E. de M., Correa, A.C., Manzoli, A., Leite, F. de L., Oliveira, C.R. de and Mattoso, L.H.C. (2010). Cellulose nanofibers from white and naturally colored cotton fibers. *Cellulose*, 17, pp. 595–606. DOI 10.1007/s10570-010-9403-0.

Torres-León, C., Rojas, R., Contreras-Esquivel, J.C., Serna-Cock, L., Belmares-Cerda, R.E. and Aguilar, C.N. (2016). Mango seed: Functional and nutritional properties. *Trends in Food Science & Technology*, *55*, pp.109-117. https://doi.org/10.1016/j.tifs.2016.06.009

Torres-León, C. *et al.* (2019) Solid-state fermentation with Aspergillus niger to enhance the phenolic

contents and antioxidative activity of Mexican mango seed: A promising source of natural antioxidants, *LWT*. Academic Press, 112, p. 108236. doi: 10.1016/j.lwt.2019.06.003.

Tunchaiyaphum, S., Eshtiaghi, M. N. and Yoswathana, N. (2013). Extraction of bioactive compounds from mango peels using green technology. *International Journal of Chemical Engineering and Applications*, 4(4), pp. 194–198. doi: 10.7763/IJCEA.2013.V4.293.

Tutt, M., Kikas, T. and Olt, J. (2012). Influence of different pretreatment methods on bioethanol production from wheat straw. *Agronomy Research Bioystem Engineeering Special*, (1), pp. 269–276.

Vijayalaxmi, S., Jayalakshmi, S.K. and Sreeramulu, K. (2014). Polyphenols from different agricultural residues: extraction, identification and their antioxidant properties *Journal of Food Science and Technology*, 52, pp. 1–9. doi: 10.1007/s13197-014-1295-9.

Warren, F.J., Gidley, M.J., Flanagen, B. (2015). Infrared spectroscopy as a tool to characterise starch ordered structure- a joint FTIR-ATR, NMR, XRD and DSC study. *Carbohydrate. Polymers* 15, pp. 1–26. https://doi.org/10.1016/j.carbpol.2015.11.066

Watkins, D., Nuruddin, M., Hosur, M., Tcherbi-narteh, A. and Jeelani, S. (2015). Extraction and characterization of lignin from different biomass resources. *Journal of Materials Research and Technology*. 4(1), pp. 26–32. doi: 10.1016/j.jmrt.2014.10.009.

Wild, P.J. De, Huijgen, W.J.J. and Heeres, H.J. (2012). Pyrolysis of wheat straw-derived organosolv lignin. *Journal of Analytical and Applied Pyrolysis*.., 93, pp. 95–103. doi: 10.1016/j.jaap.2011.10.002.

Xu, J., Krietemeyer, E.F., Boddu, V.M., Liu, S.X. and Liu, W.C. (2018) Production and characterization of cellulose nanofibril (CNF) from agricultural waste corn stover, *Carbohydrate Polymers*. Elsevier, 192(March), pp. 202–207. doi: 10.1016/j.carbpol.2018.03.017

Yingkamhaeng, N. and Sukyai, P. (2014). The potential of mango peel utilization for cellulose extraction by hydrothermal pretreatment in *The 26th Annual Meeting of the Thai Society for Biotechnology and International Conference*, pp. 101–109.

Yuan, Z., Kapu, N.S., Beatson, R., Chang, X.F. and Martinez, D.M. (2016) Effect of alkaline pre-extraction of hemicelluloses and silica on kraft pulping of bamboo (Neosinocalamus affinis Keng), *Industrial Crops and Products*. Elsevier B.V., 91, pp. 66–75. doi: 10.1016/j.indcrop.2016.06.019.

Zheng, Q., Zhou, T., Wang, Y., Cao, X., Wu, S., Zhao, M. (2018). Pretreatment of wheat straw leads to structural changes and improved enzymatic hydrolysis. *Scientific Report*s 8 (1), p.1321. https://doi.org/10.1038/s41598-018-19517-5

8 ANNEXURE

Annexure 1: Quality assessment of wheat residues for nanocellulose production using FTIR

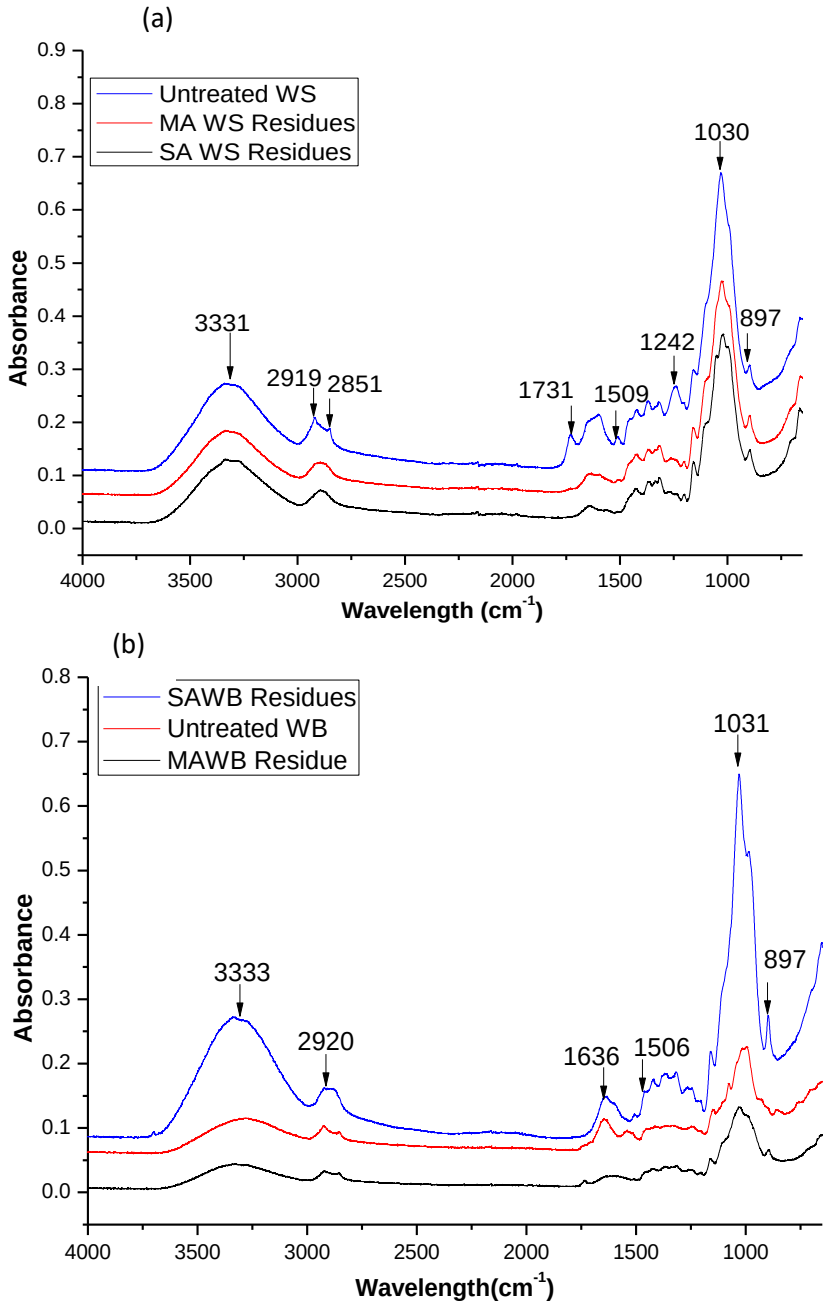

Fig A1: Effect of mild alkaline and severe alkaline on (a) wheat straw residues (MA WS residues) and (b) wheat bran residues (MA WB residues and

Annexure 2: TGA analysis of Mango Husks Hemicelluloses

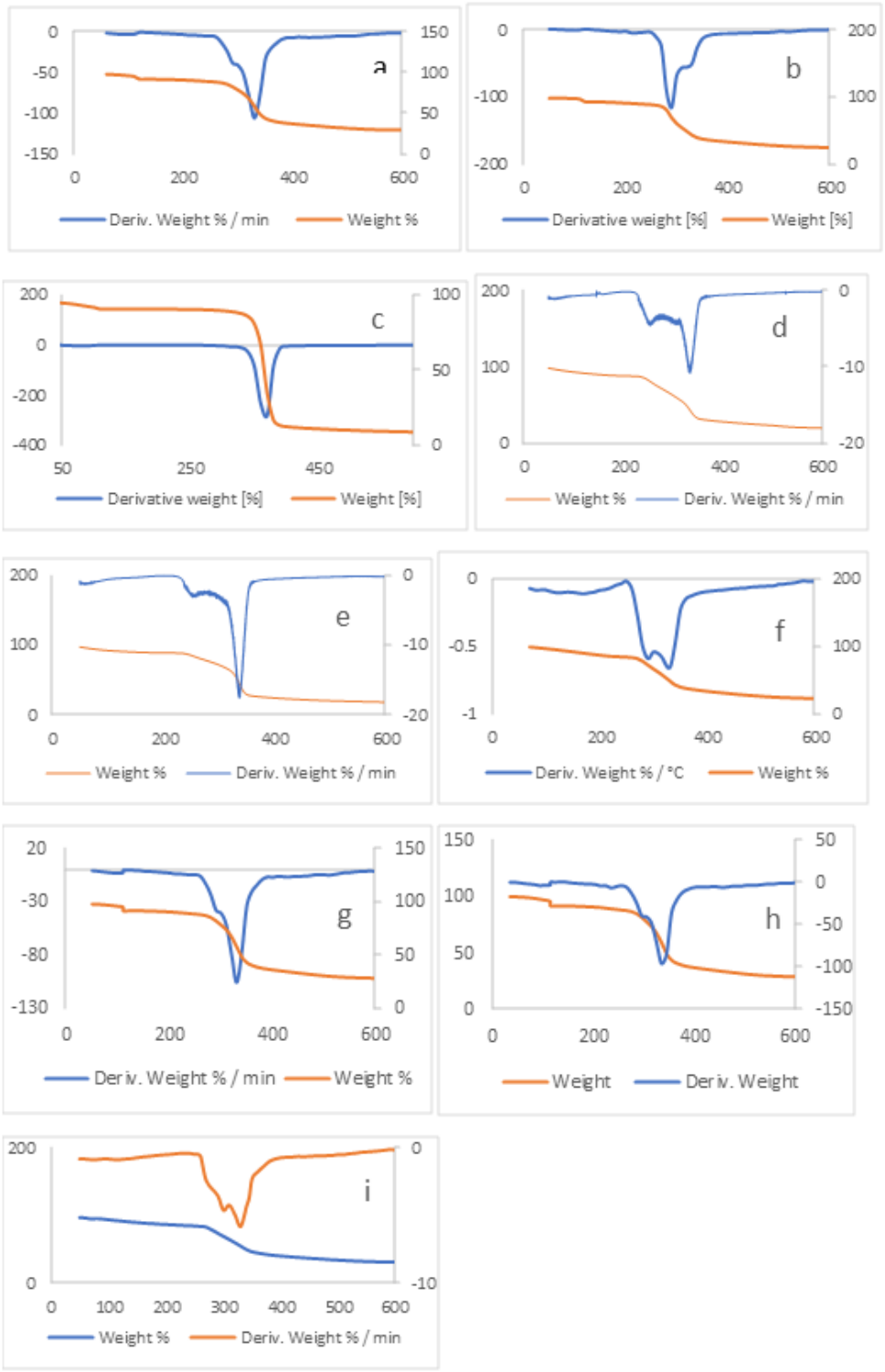

Fig. A2: TG/DTG thermographs of **a**. Mango seed husks hemicelluloses (MHH) at optimum extraction conditions, **b**. Commercial xylan (CXLN), **c**. Commercial xyloglucan (CXGN), **d.** CXGN/CXLN (0.29), **e.** CXGN/CXLN (0.47), **f.** CXGN/CXLN (0.13), **g.** MHH with XGN/XLN (0.29), **f.** MHH XGN/XLN (0.47), and **i.** MHH XGN/XLN (0.13)

Annexure 3: Links to papers published on the work:

Ceaser, R. and Chimphango, A.F., 2021. Comparative analysis of physical and functional properties of cellulose nanofibers isolated from alkaline pre-treated wheat straw in optimized hydrochloric acid and enzymatic processes. *International Journal of Biological Macromolecules*, *171*, pp.331-342. https://www.sciencedirect.com/science/article/pii/S0141813021000350?casa_token=gaM8g8KVj7cAAAAA:Eqgu8tppLGZzk1LpZbol9UYoai_1otLR0GdYn4nohcbuNZ6mZSdasfdpS0TAwHKRoKUoXbNDYfs

Mugwagwa, L.R. and Chimphango, A.F.A., 2019. Box-Behnken design based multi-objective optimisation of sequential extraction of pectin and anthocyanins from mango peels. *Carbohydrate polymers*, *219*, pp.29-38. https://www.sciencedirect.com/science/article/pii/S014486171930520X?casa_token=ZbF-LmSwvogAAAAA:-gnR4MaZ1PO6sfmUrdnE-LJNS998EcebTghBA_sBaHeK6I3BPeiONTxaru4IFOfOk5-wWxvduoc

Note: This work provided useful information to the project in terms of products that can be obtained from mango peels.

Bello, F. and Chimphango, A., 2021. Optimization of lignin extraction from alkaline treated mango seed husk by high shear homogenization-assisted organosolv process using response surface methodology. *International Journal of Biological Macromolecules*, *167*, pp.1379-1392. https://www.sciencedirect.com/science/article/pii/S0141813020350170?casa_token=ZGBd0aC2LJAAAAAA:WgARGQhQs31il_X74r_8xOYYivPFY7n4SB0ULg-bb94dxDf-emrwkI0D2PEjMso_RQuWyywOdIk

Council for Scientific and Industrial Research (CSIR)

Waste RDI Roadmap Implementation Unit

Meiring Naudé Road, Brummeria,
Pretoria, South Africa

Postal Address

PO Box 395, Pretoria, South Africa, 0001

Tel: +27 (0)12 841 4801
Fax: +27 (0)12 842 7687
Email: info@wasteroadmap.co.za

www.wasteroadmap.co.za

Department of Science and Innovation

Directorate: Environmental Services and Technologies

Meiring Naudé Road, Brummeria,
Pretoria, South Africa

Postal Address

Private Bag X894, Pretoria, South Africa, 0001

Tel: +27 (0)12 843 6300

www.dst.gov.za